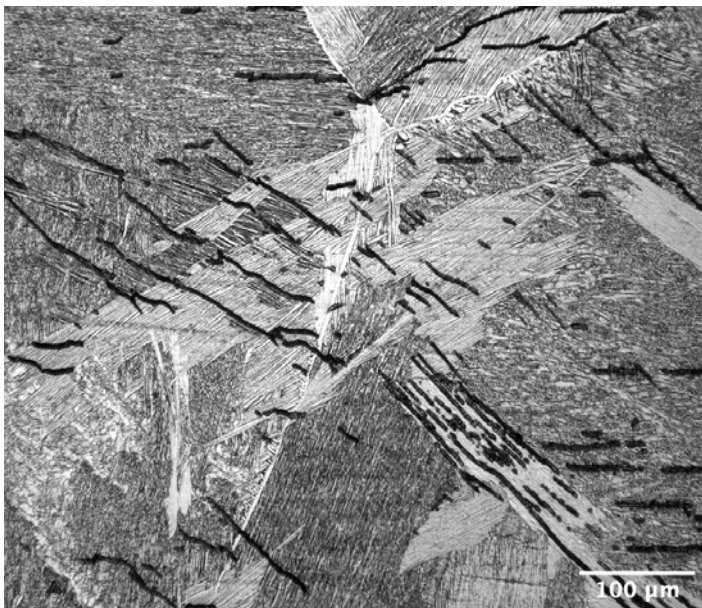




Executive summary

Fatigue of β processed and β heat-treated titanium alloys

A contribution to the DSTO - NLR joint programme of Damage Tolerance and Durability assessment of beta annealed Ti-6Al-4V plate



Report no.

NLR-TP-2009-036

Author(s)

R.J.H. Wanhill

S.A. Barter

Report classification

UNCLASSIFIED

Date

April 2009

Knowledge area(s)

Vliegtuigmateriaal- en schadeonderzoek

Descriptor(s)

Titanium alloys

Fatigue

Crack growth

Damage Tolerance

Durability

Problem area

β annealed Ti-6Al-4V ELI plate has been selected for the main wing-carry-through bulkhead and other fatigue critical structures, including the vertical tail stubs, of advanced military aircraft intended to enter service with the RAAF and the RNLAf. This titanium alloy has a chemical composition and manufacturing process intended to optimise its fatigue and fracture properties, notably in the thick sections required for large primary aircraft structure. However, little is known in detail about these

properties. Furthermore, the DSTO, RAAF and NLR have limited or no experience with this alloy.

Description of work

This report is a review of most of the available literature on the fatigue properties of β annealed Ti-6Al-4V and titanium alloys with similar microstructures. Some comparisons are made with alloys having different microstructures, in particular conventionally ($\alpha + \beta$) processed and heat-treated Ti-6Al-4V.

UNCLASSIFIED

Fatigue of beta processed and beta heat-treated titanium alloys

A contribution to the DSTO - NLR joint programme of Damage Tolerance and Durability assessment of beta annealed Ti-6Al-4V plate

Nationaal Lucht- en Ruimtevaartlaboratorium, National Aerospace Laboratory NLR

Anthony Fokkerweg 2, 1059 CM Amsterdam,
P.O. Box 90502, 1006 BM Amsterdam, The Netherlands

Telephone +31 20 511 31 13, Fax +31 20 511 32 10, Web site: www.nlr.nl

UNCLASSIFIED



NLR-TP-2009-036

Fatigue of β processed and β heat-treated titanium alloys

A contribution to the DSTO - NLR joint programme of Damage Tolerance and Durability assessment of beta annealed Ti-6Al-4V plate

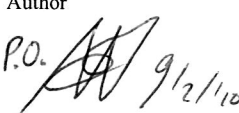


R.J.H. Wanhill and S.A. Barter¹

¹ DSTO

The contents of this report may be cited on condition that full credit is given to NLR and the authors.
This publication has been refereed by the Advisory Committee AEROSPACE VEHICLES.

Customer National Aerospace Laboratory NLR
Contract number ----
Owner National Aerospace Laboratory NLR
Division NLR Aerospace Vehicles
Distribution Unlimited
Classification of title Unclassified
January 2010

Approved by:

Author	Reviewer	Managing department
P.O.  9/12/10	 9/12/10	 9/12/10

Summary

This report is a review of most of the available literature on the fatigue properties of β annealed Ti-6Al-4V and titanium alloys with similar microstructures. The emphasis is on β processed and β heat-treated titanium alloys because β annealed Ti-6Al-4V ELI plate has been selected for the main wing-carry-through bulkhead and other fatigue critical structures, including the vertical tail stubs, of advanced military aircraft that are currently intended to enter service with the RAAF and the RNLAf. However, some comparisons are made with alloys having different microstructures, in particular conventionally ($\alpha + \beta$) processed and heat-treated Ti-6Al-4V.

Contents

1	Introduction	9
2	Microstructure of the β annealed Ti-6Al-4V ELI plate	10
3	Fatigue crack initiation	10
3.1	Microstructural initiation sites: literature	10
3.2	Microstructural initiation sites: β annealed Ti-6Al-4V ELI plate	11
3.3	Metallurgical defects	12
4	Fatigue initiation lives	13
4.1	Microstructural factors	13
4.2	Fatigue life – microstructure trends	14
4.2.1	Unnotched (smooth specimen) fatigue	15
4.2.2	Notched fatigue	16
4.3	Summary	16
5	Short/small fatigue crack growth	17
5.1	Introduction	17
5.1.1	Significance of short/small cracks	17
5.1.2	Definitions of short and small cracks	17
5.1.3	Size criteria	18
5.2	Short/small fatigue crack growth data from the literature	19
5.2.1	Coarse-grained fully lamellar IMI 685	20
5.2.2	Effects of microstructure: fully lamellar	21
5.2.3	Effects of microstructure: different types of microstructures	21
5.3	Summary	22
6	Long/large fatigue crack growth	23
6.1	Introduction	23
6.2	Fatigue thresholds	23
6.2.1	Fully lamellar microstructures	23
6.2.2	Different types of microstructures	24
6.3	Regions I and II fatigue crack growth in fully lamellar microstructures	24
6.4	Regions I and II fatigue crack growth in different types of microstructures	24

6.5	Region II bilinear $\log da/dN - \log \Delta K$ fatigue crack growth	25
6.6	Summary	25
7	Concluding remarks	26
8	References	27

Abbreviations

a	crack size
CA	Constant Amplitude
CMU	Controlling Microstructural Unit
DT&D	Damage Tolerance and Durability
EBA	Effective Block Approach
EIFS	Equivalent Initial Flaw Size
ELI	Extra Low Interstitial
EPFM	Elastic-Plastic Fracture Mechanics
FASTRAN	short crack growth model
HCF	High-Cycle Fatigue
HID	High Interstitial Defect
ISY	Intermediate Scale Yielding
K_t	stress concentration factor
LAD	Low Alloy Defect
LCF	Low-Cycle Fatigue
LEFM	Linear Elastic Fracture Mechanics
LSY	Large Scale Yielding
M	microstructural unit size
N	number of cycles
N_i	number of cycles (life) to fatigue crack initiation
N_{lc}	number of cycles (life) during long (large) fatigue crack growth
N_{sc}	number of cycles (life) during short/small fatigue crack growth
N_t	total number of cycles (fatigue life)
QF	Quantitative Fractography
r_p	crack tip plastic zone size
R	stress ratio, S_{min}/S_{max}
S	stress
S_{max}	maximum (fatigue) stress
S_{min}	minimum (fatigue) stress
SSY	Small Scale Yielding
STA	($\alpha + \beta$) Solution Treated and Aged
Y	geometric factor in LEFM description of cracks
α	titanium alloy phase with hexagonal close packed (hcp) crystal structure
β	titanium alloy phase with body centred cubic (bcc) crystal structure

ε	strain
$\Delta\varepsilon$	fatigue strain range
ΔK	stress intensity factor range
ΔK_{th}	fatigue crack growth threshold for long (large) cracks
ΔS	fatigue stress range
ΔS_e	fatigue stress range endurance limit
σ_y^c	cyclic yield stress



This page is intentionally left blank.

1 Introduction

A thick section β annealed Ti-6Al-4V ELI (Extra Low Interstitial) titanium alloy plate was purchased by the DSTO¹⁾ for investigation of its fatigue properties. This alloy has been selected for the main wing-carry-through bulkhead and other fatigue critical structures, including the vertical tail stubs, of advanced military aircraft that are currently intended to enter service with the RAAF²⁾ and the RNLAFF³⁾.

β annealed Ti-6Al-4V ELI has a chemical composition and manufacturing process intended to optimise its fatigue and fracture properties, notably in the thick sections required for large primary aircraft structure. However, little is known in detail about these properties. Furthermore, the DSTO, RAAF and NLR⁴⁾ have limited or no experience with this alloy.

Since adequate fatigue data are currently publically unavailable for β annealed Ti-6Al-4V ELI, it was proposed that the material held by DSTO be used to generate it. Owing to the common interest, the DSTO and NLR have agreed to a joint programme of testing, crack growth modelling and the development of Damage Tolerance and Durability assessment methods for this material. In addition, the DSTO requires specific data to assess the applicability of crack growth tools developed for the F/A-18 aircraft to this material. These data require a limited amount of specialised testing and crack analysis outside the current standard fatigue analysis methods.

Three fatigue life assessment methods will be considered in the joint programme:

- Strain-based fatigue crack initiation analysis, used to estimate the durability lifetime.
- Fracture mechanics based fatigue crack growth analysis, used both for damage tolerance life calculations and residual strength checks.
- Fracture mechanics based fatigue crack growth analysis, using spectrum blocks rather than constant amplitude cycles, down into the small crack regime to extend the damage tolerance prediction capability to *effective* crack initiation.

These three methods are highlighted in table 1, which is a survey of fatigue life assessment methods. We note here that the combination of the Strain – Life and EBA methods, plus

1) Defence Science and Technology Organisation, Air Vehicles Division, Victoria, Australia.

2) Royal Australian Air Force.

3) Royal Netherlands Air Force.

4) National Aerospace Laboratory NLR, Aerospace Vehicles Division, The Netherlands.

consideration of different types of crack growth models, covers most of the items in the holistic approach.

In view of the joint programme it is worthwhile to review what is available in the open literature about the fatigue properties of β annealed Ti-6Al-4V and titanium alloys with similar microstructures. This is the main subject of the present report. The topics to be considered are the microstructure of the β annealed Ti-6Al-4V ELI plate, fatigue initiation mechanisms, fatigue initiation lives, and short-to-long (or small-to-large) fatigue crack growth. Some comparisons are made with alloys having different microstructures, in particular conventionally ($\alpha + \beta$) processed and heat-treated Ti-6Al-4V.

2 Microstructure of the β annealed Ti-6Al-4V ELI plate

The β annealed Ti-6Al-4V ELI plate has a thickness of 125 mm. Figure 1 gives an example of the microstructure near the mid-thickness of the plate. β annealing resulted in a fully lamellar microstructure consisting of large colonies of aligned α platelets (Widmanstätten α) within the prior β grains. A preliminary survey of the prior β grain size (25 measurements) showed that it ranged from about 0.2 mm to 2 mm, with a mean of 1.2 mm.

The aligned α platelets are separated by thin “ribs” of remanent β . These ribs are ineffective barriers to slip, since crystallographic parallelism is possible in each colony of α platelets and interspersed β (Newkirk and Geisler 1953; Williams *et al.* 1954). However, the colonies themselves have differing crystallographic orientations and are *generally* effective barriers to slip, as are the prior β grain boundaries. These caveats are discussed in subsection 3.2.

3 Fatigue crack initiation

3.1 Microstructural initiation sites: literature

Fatigue studies of several titanium alloys with fully lamellar or duplex (equiaxed primary $\alpha +$ lamellar) microstructures have shown that crack initiation in the lamellar microstructures occurs mainly across colonies of aligned α platelets (Wells and Sullivan 1969; Eylon and Pierce 1976; Eylon and Hall 1977; Postans and Jeal 1977; Ruppen *et al.* 1979; Bania *et al.* 1982; Wojcik *et al.* 1988; Dowson *et al.* 1992; Evans and Bache 1994; Lütjering *et al.* 1996; Wagner 1996; Hines and Lütjering 1999).

The resulting microcracks are faceted with cleavage-like appearances, as are microcracks that initiate in equiaxed primary α (Neal and Blenkinsop 1976). Although these faceted cracks were initially thought to be due to cleavage, it is now more or less accepted that they are caused by intense shear in $\{0002\}$ slip bands (Wojcik *et al.* 1988; Evans and Bache 1994; Bache *et al.* 1998).

Under constant amplitude (CA) fatigue loading the faceted cracks provide no evidence of cyclic crack growth, e.g. fatigue striations. However, fatigue crack growth tests using CA + intermittent spike loading result in progression markings within single facets (Paton *et al.* 1976; Pilchak *et al.* 2009). These progression markings demonstrate that the facets developed during many loading cycles.

Other types of initiation sites have been reported: (a) microcracks at the interfaces between α platelets and remanent β , especially at prior β grain boundaries (Stubington and Bowen 1974); and (b) along the boundaries between aligned α platelets and primary α (Wells and Sullivan 1969).

3.2 Microstructural initiation sites: β annealed Ti-6Al-4V ELI plate

Some preliminary Low-Cycle Fatigue (LCF) tests were done on cylindrical specimens machined from the β annealed Ti-6Al-4V ELI plate. After testing, the surface of one of the specimens was polished and etched to reveal the microstructural locations of surface microcracks. Optical images of the microcracks were obtained using a deep focus image processing technique developed by the DSTO (Goldsmith 2000). Figure 2 shows some examples.

Most of the microcracks initiated across colonies of aligned α platelets, as would be expected from previous studies, see subsection 3.1. Some of these cracks extended with little or no deflection across two or more colonies and their boundaries, and a few also crossed the grain boundary α . There were also cracks along the interfaces between α platelets and remanent β , including colony boundaries; and at least one crack ran along the interface between grain boundary α and colonies of aligned α platelets (near the top right corner of figure 2).

Since some microcracks can cross colony boundaries and prior β grain boundaries with little or no deflection, we may infer from the studies by Wojcik *et al.* (1988), Evans and Bache (1994) and Bache *et al.* (1998) that these boundaries are not always effective barriers to slip.

3.3 Metallurgical defects

The occurrence of inclusion-type defects in ingot metallurgy titanium alloys is rare, mainly because the ingots are obtained using high purity materials and multiple vacuum-arc melting. Titanium powder compacts are, however, susceptible to inclusion defects because of powder contamination by foreign particles that are not subsequently melted (Kerr *et al.* 1976).

Costa *et al.* (1990) reviewed LCF failures due to metallurgical defects in ingot metallurgy and ($\alpha + \beta$) processed titanium aeroengine discs. Figure 3 classifies the defect types and categories and their relative frequency of occurrence in 22 in-service discs:

- (1) Type I defects are regions of α phase stabilised by high concentrations of the interstitial elements nitrogen and oxygen (sometimes called HIDs = High Interstitial Defects). Category 1 defects are very hard and brittle; category 2 defects have lower hardness, but still higher than that of the matrix. The sources of type I defects are high melting point particles of titanium nitride, titanium oxide or complex oxynitride coming from titanium sponge (“burnt” sponge), master alloy additions or revert (recycled) material.
- (2) Type II defects are regions containing an excessive amount of primary α that is abnormally stabilised by segregation of metallic elements, notably aluminium or titanium. Category 3 defects have hardnesses only slightly above that of the matrix; category 4 defects can have very low hardness (these are sometimes called LADs = Low Alloy Defects).

While very informative, it is important to put the foregoing information into perspective. Titanium disc failures are rare: of the six engine manufacturers visited by Costa’s Review Team, four had a combined total of 25 discs that cracked or failed in service owing to metallurgical defects. This is a very small number set against the thousands of discs in service up to the time of the review (1990).

Furthermore, as stated at the beginning of this subsection, ingot metallurgy alloys are produced using high purity materials and multiple vacuum-arc melting. Hence it is most unlikely that fatigue-initiating metallurgical defects will be present in a premium quality material like β annealed Ti-6Al-4V ELI plate, although defects such as machining tears, weld defects and forging laps are of course possible in manufactured components.

4 Fatigue initiation lives

4.1 Microstructural factors

The fatigue life behaviour of titanium alloys depends on several microstructural factors whose importance differs for conventionally ($\alpha + \beta$) processed and heat-treated alloys and β processed and β heat-treated alloys.

For ($\alpha + \beta$) processed and heat-treated alloys the significant microstructural factors are:

- (1) Primary α grain size. A smaller primary α grain size increases the High-Cycle Fatigue (HCF) strength (Turner and Roberts 1968; Lucas and Konieczny 1971; Lucas 1973; Bowen and Stubbington 1973; Stubbington and Bowen 1974; Lütjering *et al.* 1996; Wagner 1997).

This correlation has been explained as follows. Firstly, a smaller primary α grain size results in a higher yield strength, such that higher stresses are required to initiate slip in the primary α and cause slip band fatigue cracks (Lütjering *et al.* 1996; Wagner 1997).

Secondly, any cracks that do form will be shorter and easier to arrest at the microstructural barriers provided by α/α grain boundaries (Demulsant and Mendez 1995) and $\alpha/(\alpha + \beta)$ grain boundaries in duplex microstructures (Bolingbroke and King 1986; Demulsant and Mendez 1995).

- (2) Material texture. Crystallographic alignments of primary α grains can have large effects on HCF strength (Stubbington and Bowen 1972; Bowen and Stubbington 1973; Larson and Zarkades 1976; Peters *et al.* 1984; Lütjering and Wagner 1988).

In general, the highest fatigue strength is obtained for strong textures when the {0002} planes are parallel to the principal loading direction (Peters *et al.* 1984). This orientation inhibits slip band cracking in the primary α (Lütjering and Wagner 1988).

- (3) Oxygen content and primary α hardness. Higher oxygen contents increase the yield strength and hardness of primary α (Beever and Robinson 1969; Curtis *et al.* 1969; Sargent and Conrad 1972; Williams *et al.* 1972; Robinson and Beever 1973; Yoder *et al.* 1984). This correlates with an increase in HCF strength provided that crack initiation occurs in the primary α , and not – as can occur – in aligned α platelets in duplex microstructures (Lütjering and Wagner 1988; Lütjering *et al.* 1996; Wagner 1997). See subsection 4.2.1 also.



The effect of oxygen on primary α fatigue strength is threefold. Firstly, a higher yield strength means that higher stresses are required to cause slip band fatigue cracks: see (1) above. Secondly, oxygen restricts $\{0002\}$ slip compared to $\{10\bar{1}0\}$ and $\{10\bar{1}1\}$ slip up to oxygen contents ~ 0.5 wt. % (Curtis *et al.* 1969; Sargent and Conrad 1972; Williams *et al.* 1972), and since fatigue crack initiation in primary α is largely due to intense slip on $\{0002\}$, increased oxygen content would be expected to inhibit cracking. Thirdly, increasing oxygen content changes the slip character from wavy to planar (Curtis *et al.* 1969; Williams *et al.* 1972; Kahveci and Welsch 1989). This means that cross-slip becomes more difficult, and it is well known that cross-slip promotes slip band fatigue cracking (McEvily and Johnston 1966).

For β processed and β heat-treated alloys the significant microstructural factors are:

- (4) Colony and platelet sizes. A smaller colony size increases the LCF (Eylon and Hall 1977) and HCF (Farthing 1989) strengths, and narrower aligned α platelets within the colonies especially increase the HCF fatigue strength (Wagner 1997).
- (5) Prior β grain size. A smaller prior β grain size increases the LCF and HCF strengths (Wagner 1997; Evans 1999).

The trends in (4) and (5) may be attributed firstly to less easy nucleation of slip band fatigue cracks through the aligned α platelets, since the cracks have to cross through more of the remanent β “ribs”. Secondly, any cracks that do form will sooner reach the microstructural barriers formed by colony boundaries and prior β grain boundaries, i.e. these cracks will be shorter and easier to arrest.

In view of all the foregoing microstructural factors, it is not easy to compare the fatigue strengths of conventionally ($\alpha + \beta$) processed and heat-treated alloys and β processed and β heat-treated alloys. However, some trends have been observed. These are discussed in subsection 4.2.

4.2 Fatigue life – microstructure trends

In this context the available comparisons of fatigue life data are for conventionally ($\alpha + \beta$) processed alloys subsequently ($\alpha + \beta$) or β heat-treated. In each case the cracks grew from surfaces free of significant mechanical defects.

4.2.1 Unnotched (smooth specimen) fatigue

Figures 4 – 6 compare unnotched LCF data for Ti-6Al-4V in several microstructural conditions, including the as-received mill annealed condition. The following trends may be observed:

- (1) A coarse prior β grain size (and hence larger colonies and aligned α platelets) consistently results in the lowest fatigue curve, see figures 4 and 5.
- (2) A fine prior β grain size (and hence smaller colonies and aligned α platelets) results in a fatigue curve
 - slightly lower than that of the original mill annealed microstructure, figure 4,
 - significantly lower than that of duplex microstructures containing 10 – 30 % primary α , but slightly better than that of a duplex microstructure containing 82 % primary α , figure 6.

Figures 7 and 8 show additional data for fully lamellar and duplex microstructures. These data extend the fatigue lives into the HCF regime and show fatigue curve crossovers between 10^4 and 10^5 cycles.

These trends can be explained using a rationale by Hines and Lütjering (1999). They distinguished between the LCF and HCF regimes as follows:

Under LCF conditions the key feature is the microstructural scale. Fully lamellar microstructures have much larger scales than mill annealed or duplex microstructures, and so the slip band length is much longer. This feature causes earlier fatigue crack initiation and therefore lower fatigue curves. (Note that this would be especially true for a coarse prior β grain size.)

Under HCF conditions the maximum stresses are relatively low, and the slip band length becomes less important than the intrinsic lattice resistance to dislocation motion. For duplex microstructures the lattice resistance to dislocation motion is affected by alloying element partitioning: elements such as aluminium and oxygen tend to partition into the primary α during heat treatment, thereby weakening the β matrix and the subsequent lamellar microstructure. In this way the transformed β in a duplex microstructure can be weaker than that in a fully lamellar microstructure, leading to earlier fatigue crack initiation and LCF \rightarrow HCF fatigue curve crossovers.

It is also worth noting that Lütjering *et al.* (1996) and Wagner (1997) found that larger amounts of primary α in duplex microstructures resulted in lower LCF \rightarrow HCF curves, e.g. figure 8. However, the LCF results in figure 6 are not entirely consistent with this.

4.2.2 Notched fatigue

Figures 9 and 10 are from two investigations comparing notched LCF \rightarrow HCF curves for Ti-6Al-4V in several microstructural conditions, including the as-received mill annealed conditions (Eylon and Pierce 1976; Evans 1999). These results are very interesting, not least because the trends in each figure are different:

- (1) Figure 9 shows that the notched HCF strength of a fully lamellar microstructure was much better than the notched HCF strengths of duplex or mill annealed microstructures.
- (2) Figure 10 indicates that the notched HCF strength of a mill annealed microstructure was far better than that of the other microstructures.

The explanation for these differences most probably lies in the microstructural scale. The rankings in figure 9 are probably due to the fine prior β grain size, about 0.25 mm, for the fully lamellar microstructure and large elongated primary α grains, 0.1 – 0.15 mm, in the mill annealed microstructure. On the other hand, the rankings in figure 10 are probably due to the coarse prior β grain size, about 1.5 mm, for the fully lamellar microstructure and much smaller primary α grains, 0.02 – 0.04 mm, in the mill annealed microstructure.

We note that this explanation is apparently at variance with Hines' and Lütjering's rationale for unnotched fatigue rankings, discussed in subsection 4.2.1, since they attributed only LCF rankings to the microstructural scale. However, the coarse mill annealed microstructure of the material tested by Eylon and Pierce (1976) may well be unrepresentative with respect to later mill products.

4.3 Summary

As stated earlier, it is not easy to compare the fatigue strengths of conventionally ($\alpha + \beta$) processed and heat-treated alloys and β processed and β heat-treated alloys. However, from the information in subsections 4.2.1 and 4.2.2 it appears likely that the β annealed Ti-6Al-4V ELI plate, with its rather coarse prior β grain size (averaging about 1.2 mm, see section 2) will have relatively low LCF and HCF strengths. The relatively low oxygen content of the ELI material (0.13 max. wt. % compared to 0.2 max. wt. % for normal grade Ti-6Al-4V) could also be detrimental to the HCF strength, see Starke and Lütjering (1979).

5 Short/small fatigue crack growth

5.1 Introduction

As is well known, there is considerable evidence that short/small fatigue cracks in metals grow at faster rates and lower nominal ΔK values than those characteristic of long/large cracks (Ritchie and Suresh 1983; Suresh and Ritchie 1984). In particular, short/small cracks can grow at ΔK values well below the long/large crack growth threshold, ΔK_{th} .

Short/small fatigue crack growth is a complex subject, owing to the variety of factors that can affect the crack behaviour (McClung *et al.* 1996). For many aerospace alloys the differences in fatigue crack growth behaviour between short/small cracks and long /large cracks disappear for crack sizes larger than 0.25 – 0.5 mm (Anstee 1983; Anstee and Edwards 1983). However, there are exceptions, including β processed and β heat-treated titanium alloys, as will be discussed in subsection 5.2.

5.1.1 Significance of short/small cracks

The significance of short/small fatigue cracks during the total life of a component or structure depends on whether the design and service lives are intended to be in the LCF or HCF regimes. To begin with, we may consider the fatigue life to consist of three stages:

$$N_t = N_i + N_{sc} + N_{lc} \quad (1)$$

where N_t is the total life; N_i is the life to crack initiation (sometimes contested as non-existent); N_{sc} is the life spent in growing a short/small crack; and N_{lc} is the life spent in growing a long (large) crack.

Whether or not N_i exists, most of the life is spent before entering the long (large) crack growth stage. For LCF the estimates vary from 70 – 90 % of N_t , and for HCF it can exceed 95 % of N_t , e.g. Schijve (1967), Bania *et al.* (1982), James and Knott (1985) and Demulsant and Mendez (1995).

From these estimates we may reasonably conclude that short/small crack growth should be investigated as part of a study of fatigue life assessment methods.

5.1.2 Definitions of short and small cracks

The terms “short crack” and “small crack” both appear in the literature, sometimes virtually as synonyms. However, these terms have acquired distinct meanings, particularly in the United



States (McClung *et al.* 1996). A crack defined as “short” need have only one physical dimension that is small, but a “small” crack’s dimensions are all small.

There are also different types of short or small cracks (Ritchie and Suresh 1983; McClung *et al.* 1996):

- (1) Microstructurally short or small cracks. These are cracks with one or more dimensions smaller than a characteristic microstructural dimension, usually based on the grain size. For titanium alloys this could be the primary α grain size in conventionally ($\alpha + \beta$) processed and heat-treated alloys; and the prior β grain size or colony size in β processed and β heat-treated alloys.
- (2) Mechanically short or small cracks. These are cracks with one or more dimensions smaller than characteristic mechanical dimensions. These dimensions typically define regions of plastic deformation, e.g. crack tip plastic zones or local plasticity at the roots of notches or other stress concentrations.
- (3) Physically/chemically short or small cracks. These are cracks with one or more dimensions larger than characteristic microstructural and/or mechanical dimensions that nevertheless can grow significantly faster than truly large cracks at comparable ΔK values.

There is general agreement about the nomenclature for types (1) and (2). Whether type (3) should be called *physically* or *chemically* short or small is not entirely clear, since justification for the existence of this third type depends largely on corrosion fatigue results, see Ritchie and Suresh (1983) and McClung *et al.* (1996).

5.1.3 Size criteria

Table 2 gives suggestions for classifying small and large crack sizes according to microstructural and mechanical criteria (Taylor 1986; McClung *et al.* 1996):

- (1) Cracks are generally considered to be microstructurally small when (a) their size is less than 5 – 10 times the microstructural unit size, M , or (b) the crack tip plastic zone size is less than or equal to M . For titanium alloys M may be the primary α or prior β grain size, or the colony size, as noted in subsection 5.1.1.
- (2) Cracks often behave in a mechanically small manner when the ratio of crack size to crack tip plastic zone size is less than 4 – 20.

Another approach to describing fatigue behaviour in terms of crack size is illustrated in figure 11. This shows three regimes of fatigue behaviour: crack initiation; irregular crack growth and coalescence of any neighbouring short or small cracks; and more or less regular growth of short-to-long (or small-to-large) cracks. These three regimes are defined by both crack size and cyclic stress levels:

- Firstly, relatively high stress amplitudes that exceed the fatigue stress range endurance limit, ΔS_e , are generally necessary for crack initiation⁵⁾, and one or several microcracks may be initiated. These cracks must overcome microstructural barriers in order to grow, and are therefore classified as microstructurally short or small until they reach a certain size, a_1 , defined by the criteria in table 2 and (1) above.
- Between a_1 and a_2 , defined by the criteria in table 2 and (2) above, the cracks are classified as mechanically short or small. This means that their behaviour cannot be properly described by LEFM. As figure 11 indicates, these cracks first grow irregularly, including the coalescence of any neighbouring cracks (Demulsant and Mendez 1995). The irregular crack growth is mainly due to a persistent but lessening influence of microstructural barriers. Also it is no longer necessary that the cyclic stress amplitudes exceed ΔS_e in order to cause further cracking. This phenomenon was first reported by Kitagawa and Takahashi (1976).
- Irregular crack growth gradually gives way to nominally regular crack growth, which depends both on crack size and the cyclic stress levels: higher cyclic stress amplitudes result in transitions to regular crack growth at shorter or smaller crack sizes.
- Beyond a_2 the cracks are classified as long or large. At cyclic stress amplitudes below two-thirds of the cyclic yield stress, σ_y^c , the regular crack growth becomes amenable to description by LEFM.

5.2 Short/small fatigue crack growth data from the literature

Most of the short/small fatigue crack growth data for β processed and β heat-treated titanium alloys have been obtained for the alloy IMI 685, with some data also for IMI 829, IMI 834, Ti65S and IMI 318 (Ti-6Al-4V). There are two reasons for this selection of alloys:

- (1) Alloy composition. Table 3 gives the nominal chemical compositions of the alloys. IMI 685, IMI 829, IMI 834 and Ti65S are near- α alloys, containing predominantly α -stabilizers

⁵⁾ Crack initiation below ΔS_e occurs in some materials, e.g. carbon steels (De los Rios *et al.* 1985).

(aluminium, zirconium, and tin). They are generally β processed and/or β heat-treated, resulting in fully or partially lamellar microstructures of varying coarseness, depending on the processing conditions. On the other hand, IMI 318 (Ti-6Al-4V) is an α - β alloy, containing the α -stabilizer aluminium and a substantial amount of the β -stabilizer vanadium. α - β alloys have conventionally been ($\alpha + \beta$) processed and heat-treated, as mentioned earlier, because it is more difficult to obtain satisfactory mechanical properties from β processing and/or β heat-treating (Coyne 1970; Green and Minton 1970; Donachie 2000).

- (2) Precedence. IMI 685 was the first near- α alloy to be used in the fully lamellar condition, and so its fatigue crack growth properties were of pioneering importance.

5.2.1 Coarse-grained fully lamellar IMI 685

Figures 12 and 13 compare microstructurally short fatigue crack growth data with a long crack growth curve for coarse-grained IMI 685 (Hicks and Brown 1982; Brown and Hicks 1983; Hicks *et al.* 1983a). The cracks were up to 3.5 mm long, while the prior β grain size and colony size were about 5 mm and 1 mm respectively. Although the short crack data encompasses wide ranges in crack growth rates, there are clear trends:

- Crystallographic crack growth across aligned α platelets tended to be faster than non-crystallographic crack growth and cracking along colony boundaries and α/β interfaces.
- Short crack growth could be more than two orders of magnitude faster than long crack growth at similar ΔK values, particularly when close to the long crack growth threshold, which was $8.7 \text{ MPa}\sqrt{\text{m}}$ for $R = 0.33$ (Brown and Hicks 1983).

Hicks and Brown (1982) also observed that although the short cracks arrested (briefly) at grain and colony boundaries, they did not slow down before arresting.

More detail about crystallographic crack growth in IMI 685 was obtained from extremely coarse-grained IMI 685 that had been β heat-treated for 7 days followed by slow cooling (Bache *et al.* (1998); Wilson *et al.* 1999). The prior β grain size was about 30 mm and the colony sizes ranged from 0.1 – 5 mm. Thin (2 mm) coupons containing 0.25 mm edge notches were fatigued to through-crack lengths of about 4 mm. During the first 0.5 mm of cracking the growth rates depended strongly on the crystallographic orientation of the initially cracking colony with respect to the principal stress axis. Once the cracks grew beyond the initial colony, at about 1 – 1.5 mm *total* length, the growth rates gradually converged to similar values.

5.2.2 Effects of microstructure: fully lamellar

Three trends have been reported or proposed for the effects of fully lamellar microstructural variations on short/small fatigue crack growth over similar ranges of ΔK :

- Finer prior β grain size reduces the crack growth rates (Hastings *et al.* 1987). This conclusion was obtained from a crude comparison of small crack growth rate data for IMI 685, grain size ~ 5 μm (Brown and Hicks 1983) and Ti65S, grain size ~ 1.5 μm (Hastings *et al.* 1987). A more representative comparison is given in figure 14, which shows the data envelopes for microstructurally short crack growth across aligned α platelets. There is indeed a trend of lower crack growth rates for the finer-grained material, but there is also considerable overlap.
- A “basketweave”⁶⁾ microstructure results in lower crack growth rates than colonies of aligned α platelets (Hastings *et al.* 1987). This conclusion was based on the data in figure 15, notably a comparison of the data for crack sizes within the colony size range of the aligned microstructure. The data scatter makes this conclusion dubious, and it is also not supported by long/large fatigue crack growth rate data, see subsection 6.3.
- A finer lamellar microstructure results in lower crack growth rates than a coarse lamellar microstructure (Wagner and Lütjering 1987). This conclusion was based on the data in figure 16. The data scatter makes this conclusion somewhat dubious, but the highest overall growth rates do occur in the coarse lamellar material.

5.2.3 Effects of microstructure: different types of microstructures

Three trends have been reported or proposed for the effects of different types of microstructures on short/small fatigue crack growth over similar ranges of ΔK :

- Equiaxed primary α microstructures result in lower crack growth rates than coarse lamellar microstructures (Hicks and Brown 1984; Wagner and Lütjering 1987). This conclusion was obtained from the data shown in figures 17 and 18. The data scatter in figure 18 makes this conclusion dubious for fatigue crack growth at $R = -1$.
- Under reversed fatigue stressing ($R = -1$) equiaxed primary α microstructures result in lower crack growth rates than duplex and fine lamellar microstructures at ΔK values less than 5 $\text{MPa}\sqrt{\text{m}}$ and 10 $\text{MPa}\sqrt{\text{m}}$, respectively (Wagner and Lütjering 1987). This conclusion

⁶⁾ “Basketweave” microstructures in titanium alloys consist of fine Widmanstätten configurations of intersecting α platelets within the prior β grains.

was based on the data shown in figures 16, 18 and 19. The data scatter in these figures makes this conclusion dubious.

- Duplex microstructures result in lower crack growth rates than coarse or fine lamellar microstructures (Wagner and Lütjering 1987; Dowson *et al.* 1992; Lütjering *et al.* 1993). This conclusion was based mainly on data shown in figures 16, 19 and 20. Figure 19 partially supports this conclusion, namely for ΔK values *above* 10 MPa $\sqrt{\text{m}}$. However, figure 20 shows an opposing trend: generally lower crack growth rates occur in duplex microstructures only for ΔK values *below* 10 MPa $\sqrt{\text{m}}$.

The discrepancies between the reported or proposed trends and what figures 16, 18 – 20 indicate is due to data interpretation. Wagner and Lütjering reduced their data plots to “best fit” lines, thereby discounting the data scatter. Dowson *et al.* did this also for IMI 685 and Ti65S.

Wagner and Lütjering (1987) and Dowson *et al.* (1992) provided similar explanations of the trends derived from their “best fit” lines. They concluded that finer grain sizes and phase dimensions increase the number of microstructural barriers and improve the resistance to short/small crack growth. This explanation certainly has merit, but the data scatter shown in figures 16, 18 – 20 indicate that other factors should be considered. One likely possibility is the effect of local crystallographic orientation on the nucleation and early growth of cracks, already discussed in subsection 5.2.1, and also mentioned by Brown and Taylor (1984) and Bache (1999).

5.3 Summary

As mentioned at the beginning of subsection 5.1, short/small fatigue crack growth is a complex subject, since a variety of factors can affect the crack behaviour. In particular, the microstructures of titanium alloys can strongly influence early crack growth, with some clear trends and other not-so-clear trends, see subsection 5.2.

Many, or most, aerospace alloys have average grain sizes less than about 50 μm . In view of the criteria in table 2, this approximate grain size limit implies that microstructurally short/small fatigue crack growth behaviour should not persist beyond 0.5 mm. However, β processed and β heat-treated titanium alloys can have rather coarse microstructures. For example, the β annealed Ti-6Al-4V ELI plate that provides the motivation for this report has a prior β grain size averaging about 1.2 mm. For such coarse microstructures short/small fatigue crack growth behaviour may be expected to persist to crack sizes of several millimetres, owing to the strong

influences of the local crystallographic orientations of grains and colonies of aligned α platelets. These influences are also responsible for wide variations in crack growth rates.

The persistence and variability of short/small fatigue crack growth behaviour in coarse-grained titanium alloys demonstrate that it must be investigated as part of a study of fatigue life assessment methods for the β annealed Ti-6Al-4V ELI plate.

6 Long/large fatigue crack growth

6.1 Introduction

Long/large fatigue crack growth under constant amplitude loading can be considered in terms of the three regions shown in figure 21. In region I there is a threshold value, ΔK_{th} , below which cracks do not propagate. Above this value the crack growth rate increases relatively rapidly with increasing ΔK . In region II there is a more or less linear log-log relation between da/dN and ΔK . In region III the crack growth rate curve rises rapidly towards final failure.

Only regions I and II will be discussed in this report. For titanium alloys region II is often characterized by bilinear log-log relations between da/dN and ΔK (Yoder *et al.* 1977a, 1978, 1979, 1984; Gross *et al.* 1988; Wanhill *et al.* 1989; Saxena and Malakondaiah 1989; Ravichandran 1991; Wanhill and Looije 1993; Saxena and Radhakrishnan 1998; Wang and Müller 1998).

6.2 Fatigue thresholds

6.2.1 Fully lamellar microstructures

Figure 22 shows ΔK_{th} values for β annealed Ti-6Al-4V as functions of aligned α colony size and R. Although the data are limited, figure 22a indicates that ΔK_{th} is fairly independent of α colony size. Ravichandran (1991) provided a detailed explanation of this result. He concluded that there was a change in the microstructural units controlling crack growth and threshold. For fast-cooled fine lamellar microstructures (“basketweave”) the controlling microstructural unit (CMU) is the colony size; for relatively slow-cooled coarse lamellar microstructures (aligned α platelets) the CMU is the α platelet thickness.

Figure 23 shows ΔK_{th} values for β processed and annealed IMI 685 (Hicks *et al.* 1983b). The values for the coarsest (α colony size 0.21 mm) and finest (“basketweave”) microstructures

provide support for ΔK_{th} being fairly independent of α colony size. However, some of the data for the intermediate microstructure (α colony size 0.11 mm) are significantly lower.

Both figure 22b and figure 23 show a trend of more or less continuously decreasing ΔK_{th} with increasing R. This agrees with a general trend for titanium alloys with different types of microstructures (Chan 2004).

6.2.2 Different types of microstructures

Table 4 gives estimated ΔK_{th} values for different Ti-6Al-4V microstructures. The estimates were obtained by extrapolation of near-threshold crack growth data (Irving and Beevers 1974; Wagner and Lütjering 1987) down to a crack growth rate of 10^{-10} m/cycle. Although limited in number, the estimates are for widely different R and show that coarse lamellar microstructures had the highest ΔK_{th} values, duplex microstructures were intermediate, and equiaxed primary α microstructures (usually the mill annealed condition) had the lowest ΔK_{th} values.

6.3 Regions I and II fatigue crack growth in fully lamellar microstructures

Figures 24 and 25 compare regions I and II long/large fatigue crack growth in coarse lamellar and “basketweave” β annealed Ti-6Al-4V and β processed and annealed IMI 685. For both alloys the near-threshold crack growth rates were very similar at the same or similar R values. These results are important because they imply that near-threshold long/large fatigue crack growth in β processed and β heat-treated titanium alloys is insensitive to variations in α colony size. This adds further support to Ravichandran’s hypothesis that a change in the CMU is responsible for the similar crack growth behaviour, see subsection 6.2.1.

6.4 Regions I and II fatigue crack growth in different types of microstructures

Figures 26 – 28 compare regions I and II long/large fatigue crack growth in different microstructures of Ti-6Al-4V and another α - β alloy, Ti-6Al-4Mo-2Zr-0.2Si. The coarse and fine lamellar microstructures tend to result in the lowest crack growth rates until da/dN values of about 10^{-7} m/cycle are exceeded. The crack growth rate curves for the other types of microstructures show varying amounts of overlap.

The lower fatigue crack growth rates in fully lamellar microstructures have been attributed to extensive crack branching and deflection (Yoder *et al.* 1976, 1977a, 1977b; Eylon and Bania 1978; Eylon 1979; Bania *et al.* 1982) and enhanced roughness-induced fatigue crack closure (Halliday and Beevers 1981; Hicks *et al.* 1983b; Saxena and Radhakrishnan 1998). Both these characteristics lower the fatigue crack driving force (Suresh and Ritchie 1982; Suresh 1983, 1985).

6.5 Region II bilinear log da/dN – log ΔK fatigue crack growth

As mentioned in subsection 6.1, region II fatigue crack growth in titanium alloys is often characterized by bilinear log – log relations between da/dN and ΔK. Figure 29 gives examples for (a) a β annealed Ti-6Al-4V ELI plate and (b) several alloys in different heat treatment conditions (Yoder *et al.* (1978, 1979). Figure 29a indicates the transition point, T, where the bilinear relation changes slope. Figure 29b shows a very wide data band, with a 50-fold difference in crack growth rates at ΔK = 21 MPa√m.

The transition points in the bilinear plots (T in figure 29a) correspond to changes in fatigue fracture topography. For all these alloys crack growth was predominantly structure-sensitive, involving crack branching and deflection, in the hypotransitional region IIa; and predominantly structure-insensitive, more or less continuum-mode fracture, in the hypertransitional region IIb.

Much attention has been paid to analysing these and similar results (Irving and Beevers 1974; Yoder *et al.* 1976, 1977b, 1978, 1979, 1980; Gross *et al.* 1988; Ravichandran and Dwarakadasa 1989; Wanhill *et al.* 1989; Wanhill and Looije 1993; Wang and Müller 1998). It was variously concluded that the transitions occur at ΔK values where either the monotonic or cyclic plastic zone sizes at the crack tips attain and exceed the average CMU dimensions; and the CMUs could be the primary α grain size, the fine or coarse lamellar α colony size, or the coarse lamellar α platelet thickness.

Be that as it may, an important practical point is that structure-sensitive to structure-insensitive transitions in titanium alloys can also occur under variable amplitude loading (Wanhill and Looije 1993). Wanhill *et al.* (1989) and Wanhill and Looije (1993) predicted that visible transitions on service fatigue fractures would provide “benchmarks” for analysing local stress and stress intensity factor conditions, thereby assisting in the overall analysis of service problems. This prediction was confirmed during investigation of a Ti-6Al-4V helicopter rotor hub failure (Wanhill 2003).

6.6 Summary

Long/large fatigue crack growth in titanium alloys is in general a complex subject. This is exemplified by the detailed analyses of region II crack growth mentioned in subsection 6.5. However, the fatigue threshold and near-threshold fatigue crack growth data for β processed and β heat-treated titanium alloys suggest that variations in α colony size have little effect, see subsections 6.2.1 and 6.3. This is important with respect to the β annealed Ti-6Al-4V ELI plate that provides the motivation for this report. The plate’s thickness of 125 mm may be expected to

result in some variations in α colony size, but this is unlikely to significantly affect the fatigue threshold and near-threshold fatigue crack growth behaviour.

Another important aspect is the structure-sensitive to structure-insensitive transition during region II fatigue crack growth. The ΔK value for this transition may show some variation through the plate thickness. The fracture topography characteristics of this transition should be determined. As pointed out in subsection 6.5, the transition can act as a “benchmark” for fracture mechanics analyses of service failures.

7 Concluding remarks

This report is a review of most of the available literature on the fatigue properties of β annealed Ti-6Al-4V and titanium alloys with similar microstructures. The focus is on β processed and β heat-treated titanium alloys. This is because β annealed Ti-6Al-4V ELI plate has been selected for the main wing-carry-through bulkhead and other fatigue critical structures, including the vertical tail stubs, of advanced military aircraft currently intended to enter service with the RAAF and the RNLAf. However, some comparisons are made with alloys having different microstructures, in particular conventionally ($\alpha + \beta$) processed and heat-treated Ti-6Al-4V.

The review has been necessarily limited to fatigue under constant amplitude loading. There appears to be no open-source literature on the fatigue behaviour of β processed and β heat-treated titanium alloys under variable amplitude loading, in particular load histories representative for military airframe components. Also, nothing is known about the ability of constitutive and crack growth models to predict this behaviour.

This situation emphasizes the practical usefulness of the DSTO – NLR programme to develop Damage Tolerance and Durability assessment methods for β annealed Ti-6Al-4V ELI plate.

8 References

1. Anstee, R.F.W. (1983): An assessment of the importance of small crack growth to aircraft design, *Behaviour of Short Cracks in Aircraft Components*, AGARD Conference Proceedings No. 328, Advisory Group for Aerospace Research and Development, Neuilly-sur-Seine, France, pp. 3-1–3-9.
2. Anstee, R.F.W., Edwards, P.R. (1983): A review of crack growth threshold and crack propagation rates at short crack lengths, *Some Considerations on Short Crack Growth Behaviour in Aircraft Structures*, AGARD Report No. 696, Advisory Group for Aerospace Research and Development, Neuilly-sur-Seine, France, pp. 2-1–2-12.
3. Bache, M.R. (1999): Microstructural influences on fatigue crack growth in the near alpha titanium alloy Timetal 834, *Small Fatigue Cracks: Mechanics, Mechanisms and Applications*, Editors K.S. Ravichandran, R.O. Ritchie and Y. Murakami, Elsevier Science Ltd., Oxford, UK, pp. 179-186.
4. Bache, M.R., Evans, W.J., Randle, V., Wilson, R.J. (1998): Characterization of mechanical anisotropy in titanium alloys, *Materials Science and Engineering A*, Vol. A257, pp. 139-144.
5. Bania, P.J., Bidwell, L.R., Hall, J.A., Eylon, D., Chakrabarti, A.K. (1982): Fracture – microstructure relationships in titanium alloys, *Titanium and Titanium Alloys, Scientific and Technological Aspects*, Editors J.C. Williams and A.F. Belov, Plenum Press, New York, USA, Vol. 1, pp. 663-677.
6. Beevers, C.J., Robinson, J.L. (1969): Some observations on the influence of oxygen content on the fatigue behaviour of α -titanium, *Journal of the Less-Common Metals*, Vol. 17, pp. 345-352.
7. Bolingbroke, R.K., King, J.E. (1986): The growth of short fatigue cracks in titanium alloys IMI550 and IMI318, *Small Fatigue Cracks*, Editors R.O. Ritchie and J. Lankford, The Metallurgical Society, Inc., Warrendale, USA, pp. 129-144.
8. Bowen, A.W., Stubbington, C.A. (1973): The effect of $\alpha + \beta$ working on the fatigue and tensile properties of Ti-6Al-4V bars, *Titanium Science and Technology*, Editors R.I. Jaffee and H.M. Burte, Plenum Press, New York, USA, Vol. 3, pp. 2097-2108.
9. Brown, C.W., Hicks, M.A. (1983): A study of short fatigue crack growth behaviour in titanium alloy IMI 685, *Fatigue of Engineering Materials and Structures*, Vol. 6, pp. 67-76.
10. Brown, C.W., Taylor, D. (1984): The effects of texture and grain size on the short fatigue crack growth rates in Ti-6Al-4V, *Fatigue Crack Growth Threshold Concepts*, Editors D.L. Davidson and S. Suresh, The Metallurgical Society of AIME, Warrendale, USA, pp. 433-446.

11. Chan, K.S. (2004): Variability of large-crack fatigue-crack-growth thresholds in structural alloys, *Metallurgical and Material Transactions A*, Vol. 35A, pp. 3721-3735.
12. Costa, J.G., Gonzalez, R.E., Guyotte, R.E., Salvano, D.P., Swift, T., Koenig, R.J. (1990): Titanium Rotating Components Review Team Report, United States of America Federal Aviation Administration, Aircraft Certification Service, Engine and Propeller Directorate.
13. Coyne, J.E. (1970): The beta forging of titanium alloys, *The Science, Technology and Application of Titanium*, Editors R.I. Jaffee and N.E. Promisel, Pergamon Press, London, UK, pp. 97-110.
14. Curtis, R.E., Boyer, R.R., Williams, J.C. (1969): Relationship between composition, microstructure, and stress corrosion cracking (in salt solution) in titanium alloys, *Transactions of the ASM*, Vol. 62, pp. 457-469.
15. De los Rios, E.R., Mohamed, H.J., Miller, K.J. (1985): A micromechanics analysis for short fatigue crack-growth, *Fatigue and Fracture of Engineering Materials and Structures*, Vol. 8, pp. 49-63.
16. Demulsant, X., Mendez, J. (1995): Microstructural effects on small fatigue crack initiation and growth in Ti6Al4V alloys, *Fatigue and Fracture of Engineering Materials and Structures*, Vol. 18, pp. 1483-1497.
17. Donachie, Jr., M.J. (2000): *Titanium: A Technical Guide*, Second Edition, ASM International, Materials Park, USA, pp. 34-37.
18. Dowson, A.L., Hollis, A.C., Beevers, C.J. (1992): The effect of the alpha-phase volume fraction and stress ratio on the fatigue crack growth characteristics of the near-alpha IMI 834 Ti alloy, *International Journal of Fatigue*, Vol. 14, pp. 262-270.
19. Evans, W.J. (1999): Microstructure and the development of fatigue cracks at notches, *Materials Science and Engineering A*, Vol. A263, pp. 160-175.
20. Evans, W.J., Bache, M.R. (1994): Dwell-sensitive fatigue under biaxial loads in the near-alpha titanium alloy IMI685, *International Journal of Fatigue*, Vol. 16, pp. 443-452.
21. Ewalds, H.L., Wanhill, R.J.H. (1984): *Fracture Mechanics*, Edward Arnold (Publishers) Ltd and Delftse Uitgevers Maatschappij b.v., London, UK, and Delft, the Netherlands, pp. 172-173.
22. Eylon, D. (1979): Faceted fracture in beta annealed titanium alloys, *Metallurgical Transactions A*, Vol. 10A, pp. 311-317.
23. Eylon, D., Bania, P.J. (1978): Fatigue cracking characteristics of β -annealed large colony Ti-11 alloy, *Metallurgical Transactions A*, Vol. 9A, pp. 1273-1279.
24. Eylon, D., Hall, J.A. (1977): Fatigue behavior of beta processed titanium alloy IMI 685, *Metallurgical Transactions A*, Vol. 8A, pp. 981-990.

25. Eylon, D., Pierce, C.M. (1976): Effect of microstructure on notch fatigue properties of Ti-6Al-4V, *Metallurgical Transactions A*, Vol. 7A, pp. 111-121.
26. Farthing, T.W. (1989): Titanium – The producer’s view, *Metals Fight Back Conference – Advanced Metallic Alloys for Aerospace Applications*, Shephard Conferences and Exhibitions, Slough, UK.
27. Goldsmith, N.T. (2000): Deep focus; a digital image processing techniques to produce improved focal depth in light microscopy, *Image Analysis and Stereology*, Vol. 19, pp.163-167.
28. Green, T.E., Minton, C.D.T. (1970): The effect of beta processing on properties of titanium alloys, *The Science, Technology and Application of Titanium*, Editors R.I. Jaffee and N.E. Promisel, Pergamon Press, London, UK, pp. 111-119.
29. Gross, T.S., Bose, S., Zhong, L. (1988): Frictional effects on fatigue crack growth in β -annealed Ti-6Al-4V, *Fatigue and Fracture of Engineering Materials and Structures*, Vol. 11, pp. 179-187.
30. Halliday, M.D., Beevers, C.J. (1981): Some aspects of fatigue crack closure in two contrasting titanium alloys, *Journal of Testing and Evaluation*, Vol. 9, pp.195-201.
31. Hastings, P.J., Hicks, M.A., King, J.E. (1987): The effect of α -platelet morphology and β -grain size on the initiation and growth of short fatigue cracks in Ti65S, *Fatigue '87*, Editors R.O. Ritchie and E.A. Starke, Jr., Engineering Materials Advisory Services Ltd, Warley, UK, Vol. I, pp. 251-259.
32. Hicks, M.A., Brown, C.W. (1982): Short fatigue crack growth in planar slip materials, *International Journal of Fatigue*, Vol. 4, pp.167-169.
33. Hicks, M.A., Brown, C.W. (1984): A comparison of short crack growth behaviour in engineering alloys, *Fatigue 84*, Editor C.J. Beevers, Engineering Materials Advisory Services Ltd, Warley, UK, Vol. III, pp. 1337-1347.
34. Hicks, M.A., Howland, C., Brown, C.W. (1983a): Effect of load ratio and peak stress on short fatigue crack growth in β -processed titanium alloys, *The Metallurgy of Light Alloys*, Editors R.J. Taunt and P.J. Gregson, The Institution of Metallurgists, London, UK, pp. 252-259.
35. Hicks, M.A., Jeal, R.H., Beevers, C.J. (1983b): Slow fatigue crack growth and threshold behaviour in IMI 685, *Fatigue of Engineering Materials and Structures*, Vol. 6, pp. 51-65.
36. Hines, J.A., Lütjering, G. (1999): Propagation of microcracks at stress amplitudes below the conventional fatigue limit in Ti-6Al-4V, *Fatigue and Fracture of Engineering Materials and Structures*, Vol. 22, pp. 657-665.
37. Irving, P.E., Beevers, C.J. (1974): Microstructural influences on fatigue crack growth in Ti-6Al-4V, *Materials Science and Engineering*, Vol. 14, pp.229-238.

38. James, M.N., Knott, J.F. (1985): Aspects of small crack growth, *Damage Tolerance Concepts for Critical Engine Components*, AGARD Conference Proceedings No. 393, Advisory Group for Aerospace Research and Development, Neuilly-sur-Seine, France, pp. 10-1–10-12.
39. Kahveci, A.I., Welsch, G. (1989): Effects of oxygen on phase composition and strength of Ti-6Al-4V alloy, *Proceedings of the Sixth World Conference on Titanium*, Editors P. Lacombé, R. Tricot and G. Béranger, Les Éditions de Physique, Paris, France, Vol. 1, pp. 339-343.
40. Kerr, W.R., Eylon, D., Hall, J.A. (1976): On the correlation of specific fracture surface and metallographic features by precision sectioning in titanium alloys, *Metallurgical Transactions A*, Vol. 7A, pp. 1477-1480.
41. Kitagawa, H., Takahashi, S. (1976): Applicability of fracture mechanics to very small cracks or cracks in the early stage, *Proceedings of the Second International Conference on the Mechanical Behaviour of Materials (ICM-II)*, American Society for Metals, Metals Park, USA, pp. 627-631.
42. Larson, F.R., Zarkades, A. (1976): Improved fatigue life in titanium through texture control, *Texture and the Properties of Materials*, Editors G.J. Davies, I.L. Dillamore, R.C. Hudd and J.S. Kallend, The Metals Society, London, UK, pp. 210-216.
43. Lucas, J.J. (1973): Improvements in the fatigue strength of Ti-6Al-4V forgings, *Titanium Science and Technology*, Editors R.I. Jaffee and H.M. Burte, Plenum Press, New York, USA, Vol. 3, pp. 2081-2095.
44. Lucas, J.J., Konieczny, P.P. (1971): Relationship between alpha grain size and crack initiation fatigue strength in Ti-6Al-4V, *Metallurgical Transactions*, Vol. 2, pp. 911-912.
45. Lütjering, G., Gysler, A., Albrecht, J. (1996): Influence of microstructure on fatigue resistance, *Fatigue '96*, Editors G. Lütjering and H. Nowack, Elsevier Science Ltd, Oxford, UK, Vol. II, pp. 893-904.
46. Lütjering, G., Helm, D., Däubler, M. (1993): Influence of microstructure on fatigue properties of the new titanium alloy IMI 834, *Fatigue '93*, Editors J.-P. Bailon and J.I. Dickson, Engineering Materials Advisory Services Ltd, Warley, UK, Vol. 1, pp. 165-170.
47. Lütjering, G., Wagner, L. (1988): Influence of texture on fatigue properties of titanium alloys, *Directional Properties of Materials*, Editor H.J. Bunge, DGM Informationsgesellschaft mbH, Oberursel, Germany, pp. 177-188.
48. McClung, R.C., Chan, K.S., Hudak, Jr., S.J., Davidson, D.L. (1996): Behavior of small fatigue cracks, *ASM Handbook Volume 19 Fatigue and Fracture*, Editors S.R. Lampman *et al.*, ASM International, Materials Park, USA, pp. 153-158.

49. McEvily, Jr., A.J., Johnston, T.L. (1966): The role of cross-slip in brittle fracture and fatigue, *Proceedings of the First International Conference on Fracture*, Editors T. Yokobori, T. Kawasaki and J.L. Swedlow, The Japanese Society for Strength and Fracture of Materials, Japan, Vol. 2, pp. 515-546.
50. Neal, D.F., Blenkinsop, P.A. (1976): Internal fatigue origins in α - β titanium alloys, *Acta Metallurgica*, Vol. 24, pp. 59-63.
51. Newkirk, J.B., Geisler, A.H. (1953): Crystallographic aspects of the beta to alpha transformation in titanium, *Acta Metallurgica*, Vol. 1, pp. 370-374.
52. Paton, N.E., Williams, J.C., Chesnutt, J.C., Thompson, A.W. (1976): The effects of microstructure on the fatigue and fracture of commercial titanium alloys, AGARD Conference Proceedings No. 185, Advisory Group for Aerospace Research and Development, Neuilly-sur-Seine, France, pp. 4-1-4-14.
53. Peters, M., Gysler, A., Lütjering, G. (1984): Influence of texture on fatigue properties of Ti-6Al-4V, *Metallurgical Transactions A*, Vol. 15A, pp. 1597-1605.
54. Pilchak, A.L., Bhattacharjee, A., Rosenberger, A.H., Williams, J.C. (2009): Low ΔK faceted crack growth in titanium alloys, *International Journal of Fatigue*, Vol. 31, pp. 989-994.
55. Postans, P.J., Jeal, R.H. (1977): Dependence of crack growth performance upon structure in β processed titanium alloys, *Forging and Properties of Aerospace Materials*, The Metals Society, London, UK, pp. 192-198.
56. Ravichandran, K.S. (1991): Near threshold fatigue crack growth behavior of a titanium alloy: Ti-6Al-4V, *Acta Metallurgica et Materialia*, Vol. 39, pp. 401-410.
57. Ravichandran, K.S., Dwarakadasa, E.S. (1989): Fatigue crack growth transitions in Ti-6Al-4V alloy, *Scripta METALLURGICA*, Vol. 23, pp. 1685-1690.
58. Ritchie, R.O., Suresh, S. (1983): Mechanics and physics of the growth of small cracks, *Behaviour of Short Cracks in Aircraft Components*, AGARD Conference Proceedings No. 328, Advisory Group for Aerospace Research and Development, Neuilly-sur-Seine, France, pp. 1-1-1-14.
59. Robinson, J.L., Beevers, C.J. (1973): The effects of load ratio, interstitial content, and grain size on low-stress fatigue-crack propagation in α -titanium, *Metal Science Journal*, Vol. 7, pp. 153-159.
60. Ruppen, J., Bhowal, P., Eylon, D., McEvily, A.J. (1979): On the process of subsurface fatigue crack initiation in Ti-6Al-4V, *Fatigue Mechanisms*, ASTM STP 675, Editor J. Fong, American Society for Testing and Materials, Philadelphia, USA, pp. 47-68.
61. Sargent, G.A., Conrad, H. (1972): On the strengthening of titanium by oxygen, *Scripta METALLURGICA*, Vol. 6, pp. 1099-1101.

62. Saxena, V.K., Malakondaiah, G. (1989): Effect of heat treatment on fatigue crack growth in Ti-6Al-3.5Mo-1.9Zr-0.23Si alloy, *International Journal of Fatigue*, Vol. 11, pp. 423-428.
63. Saxena, V.K., Radhakrishnan, V.M. (1998): Effect of phase morphology on fatigue crack growth behavior of α - β titanium alloy – a crack closure rationale, *Metallurgical and Material Transactions A*, Vol. 29A, pp. 245-261.
64. Schijve, J. (1967): Significance of fatigue cracks in micro-range and macro-range, *Fatigue Crack Propagation, ASTM STP 415*, Editors J.C. McMillan and R.M.N. Pelloux, American Society for Testing and Materials, Philadelphia, USA, pp. 415-459.
65. Starke, Jr., E.A., Lütjering, G. (1979): Cyclic plastic deformation and microstructure, *Fatigue and Microstructure*, American Society for Metals, Metals Park, USA, pp. 205-243.
66. Stubbington, C.A., Bowen, A.W. (1972): The effect of section size on the fatigue properties of Ti-6Al-4V bars, Royal Aircraft Establishment Technical Report TR72091, Procurement Executive, Ministry of Defence, Farnborough, UK.
67. Stubbington, C.A., Bowen, A.W. (1974): Improvements in the fatigue strength of Ti-6Al-4V through microstructure control, *Journal of Materials Science*, Vol. 9, pp. 941-947.
68. Suresh, S. (1983): Crack deflection: implications for the growth of long and short fatigue cracks, *Metallurgical Transactions A*, Vol.14A, pp. 2375-2385.
69. Suresh, S. (1985): Fatigue crack deflection and fracture surface contact: micromechanical models, *Metallurgical Transactions A*, Vol. 16A, pp. 249-259.
70. Suresh, S., Ritchie, R.O. (1982): A geometrical model for fatigue crack closure induced by fracture surface morphology, *Metallurgical Transactions A*, Vol.13A, pp. 1627-1631.
71. Suresh, S., Ritchie, R.O. (1984): The propagation of short fatigue cracks, *International Metallurgical Reviews*, Vol. 29, pp. 445-476.
72. Taylor, D. (1986): Fatigue of short cracks: the limitations of fracture mechanics, *The Behaviour of Short Fatigue Cracks*, Editors K.J. Miller and E.R. de los Rios, Mechanical Engineering Publications, London, UK, pp. 479-490.
73. Turner, N.G., Roberts, W.T. (1968): Fatigue behavior of titanium, *Transactions of the Metallurgical Society of AIME*, Vol. 242, pp. 1223-1230.
74. Wagner, L. (1997): Fatigue life behavior, *ASM Handbook Volume 19 Fatigue and Fracture*, Editors S.R. Lampman *et al.*, Second Printing, ASM International, Materials Park, USA, pp. 837-845.
75. Wagner, L., Lütjering, G. (1987): Microstructural influence on propagation behavior of short cracks in an (α + β) Ti alloy, *Zeitschrift für Metallkunde*, Vol. 78, pp. 369-375.

76. Wang, S.-H., Müller, C. (1998): A study on the change of fatigue fracture mode in two titanium alloys, *Fatigue and Fracture of Engineering Materials and Structures*, Vol. 21, pp. 1077-1087.
77. Wanhill, R.J.H. (2003): Material-based failure analysis of a helicopter rotor hub, *Practical Failure Analysis*, Vol. 3, pp. 59-69.
78. Wanhill, R.J.H., Galatolo, R., Looije, C.E.W. (1989): Fractographic and microstructural analysis of fatigue crack growth in a Ti-6Al-4V fan disc forging, *International Journal of Fatigue*, Vol. 11, pp. 407-416.
79. Wanhill, R.J.H., Looije, C.E.W. (1993): Fractographic and microstructural analysis of fatigue crack growth in Ti-6Al-4V fan disc forgings, *AGARD Engine Disc Cooperative Test Programme*, AGARD Report 766 (Addendum), Advisory Group for Aerospace Research and Development, Neuilly-sur-Seine, France, pp. 2-1-2-40.
80. Wells, C.H., Sullivan, C.P. (1969): Low-cycle fatigue crack initiation in Ti-6Al-4V, *Transactions of the ASM*, Vol. 62, pp. 263-270.
81. Williams, A.J., Cahn, R.W., Barrett, C.S. (1954): The crystallography of the β - α transformation in titanium, *Acta Metallurgica*, Vol. 2, pp. 117-128.
82. Williams, J.C., Sommer, A.W., Tung, P.P. (1972): The influence of oxygen concentration on the internal stress and dislocation arrangements in α titanium, *Metallurgical Transactions*, Vol. 3, pp. 2979-2984.
83. Wilson, R.J., Bache, M.R., Evans, W.J. (1999): Crystallographic orientation and short fatigue crack propagation in a titanium alloy, *Small Fatigue Cracks: Mechanics, Mechanisms and Applications*, Editors K.S. Ravichandran, R.O. Ritchie and Y. Murakami, Elsevier Science Ltd., Oxford, UK, pp. 199-206.
84. Wojcik, C.C., Chan, K.S., Koss, D.A. (1988): Stage I fatigue crack propagation in a titanium alloy, *Acta Metallurgica*, Vol. 36, pp. 1261-1270.
85. Yoder, G.R., Cooley, L.A., Crooker, T.W. (1976): A micromechanistic interpretation of cyclic crack-growth behavior in a beta-annealed Ti-6Al-4V alloy, NRL Report 8048, Naval Research Laboratory, Washington, D.C., USA.
86. Yoder, G.R., Cooley, L.A., Crooker, T.W. (1977a): Enhancement of fatigue crack growth and fracture resistance in Ti-6Al-4V and Ti-6Al-6V-2Sn through microstructural modification, *Transactions of the ASME, Journal of Engineering Materials and Technology*, Vol. 99, pp. 313-318.
87. Yoder, G.R., Cooley, L.A., Crooker, T.W. (1977b): Observations on microstructurally sensitive fatigue crack growth in a Widmanstätten Ti-6Al-4V alloy, *Metallurgical Transactions A*, Vol. 8A, pp. 1737-1743.



88. Yoder, G.R., Cooley, L.A., Crooker, T.W. (1978): Fatigue crack propagation resistance of beta-annealed Ti-6Al-4V alloys of differing interstitial oxygen contents, *Metallurgical Transactions A*, Vol. 9A, pp. 1413-1420.
89. Yoder, G.R., Cooley, L.A., Crooker, T.W. (1979): 50-fold difference in region-II fatigue crack propagation resistance of titanium alloys: a grain size effect, *Transactions of the ASME, Journal of Engineering Materials and Technology*, Vol. 101, pp. 86-90.
90. Yoder, G.R., Cooley, L.A., Crooker, T.W. (1980): Observations on the generality of the grain-size effect on fatigue crack growth in $\alpha + \beta$ titanium alloys, *Titanium '80 Science and Technology*, Editors H. Kimura and O. Izumi, The Metallurgical Society of AIME, Warrendale, USA, pp. 1865-1873.
91. Yoder, G.R., Froes, F.H., Eylon, D. (1984): Effect of microstructure, strength, and oxygen content on fatigue crack growth rate of Ti-4.5Al-5.0Mo-1.5Cr (CORONA 5), *Metallurgical Transactions A*, Vol. 15A, pp. 183-197.

Table 1 Survey of fatigue life assessment methods

Assessment Methods
<ul style="list-style-type: none"> • Stress – Life (S – N) <ul style="list-style-type: none"> ○ fatigue stress range endurance limits, ΔS_e, unnotched and notched (K_t) data ○ modifications to ΔS_e ○ mean stress effects (R) ○ linear damage rule, also for variable R ○ scatter factors • Strain – Life (ϵ – N) <ul style="list-style-type: none"> ○ strain – life equation, unnotched data, $R = -1$ ○ cyclic stress – strain curve analysis ○ rainflow cycle counting (closed hysteresis loops) ○ stress – strain at critical location (notch analysis) ○ mean stress effects (R) via equivalent strain equations, leading to equivalent strain amplitudes ○ damage accumulation rule • Damage Tolerance and Durability (DT&D) <ul style="list-style-type: none"> ○ specified initial flaw sizes (EIFS) ○ back-extrapolation of long crack growth data ○ LEFM long crack growth models (non-interaction, yield zone, crack opening, strip yield) ○ possible use of crack opening model for short cracks (FASTRAN); differences in long and short crack thresholds need to be included ○ mainly deterministic: stochastic approach becoming accepted • DSTO Flight Block Spectrum Loading (Effective Block Approach, EBA) <ul style="list-style-type: none"> ○ short-to-long crack growth data using marker loads and Quantitative Fractography (QF) ○ data compilations to establish empirical crack growth “laws” ○ deterministic (“upper bound”) and stochastic approaches • Holistic <ul style="list-style-type: none"> ○ fatigue initiation mechanisms (also as functions of notch stress concentrations, K_t) ○ fatigue initiation lives (S – N and/or ϵ – N assessments) ○ evaluation and selection of marker load strategies for Quantitative Fractography (QF) of short-to-long crack growth ○ short-to-long long crack growth using marker loads and QF ○ establishment, validation and choice of appropriate crack growth models and “laws” ○ deterministic (“upper bound”) and stochastic approaches

Table 2 Size criteria for small cracks (McClung et al. 1996)

Microstructural Size	Mechanical Size	
	Large: $a/r_p > 4-20$ (SSY)	Small: $a/r_p < 4-20$ (ISY and LSY)
Large: $a/M > 5-10$ and $r_p/M \gg 1$	mechanically and microstructurally large (LEFM valid)	mechanically small but microstructurally large (may need EPFM)
Small: $a/M < 5-10$ and $r_p/M \sim 1$	mechanically large but microstructurally small	mechanically and microstructurally small

a = crack size; r_p = crack tip plastic zone size; M = microstructural unit size; SSY = Small Scale Yielding
 ISY = Intermediate Scale Yielding; LSY = Large Scale Yielding; LEFM = Linear Elastic Fracture Mechanics
 EPFM = Elastic-Plastic Fracture Mechanics

Table 3 Nominal chemical compositions of several titanium alloys (wt. %)

Near- α alloys	IMI 685	Ti-6Al-5Zr-0.5Mo-0.25Si-0.1Fe
	IMI 829	Ti-5.5Al-3Zr-3.5Sn-1Nb
	IMI 834	Ti-5.8Al-3.5Zr-4Sn-0.7Nb-0.5Mo-0.35Si-0.06C
	Ti 65S	Ti-6Al-5Zr-0.5Mo-0.25Si-0.2Fe-100ppmHf
α - β alloy	IMI 318	Ti-6Al-4V-0.15Fe-0.17O

Table 4 Estimated fatigue thresholds for Ti-6Al-4V with different microstructures

R	Microstructure	ΔK_{th} (MPa \sqrt{m})
-1	coarse lamellar	7.2
	fine lamellar	5.2
	duplex	7.2
	equiaxed primary α	4.6
0.35	coarse lamellar	5.8
	duplex	3.4
	equiaxed primary α	3.1

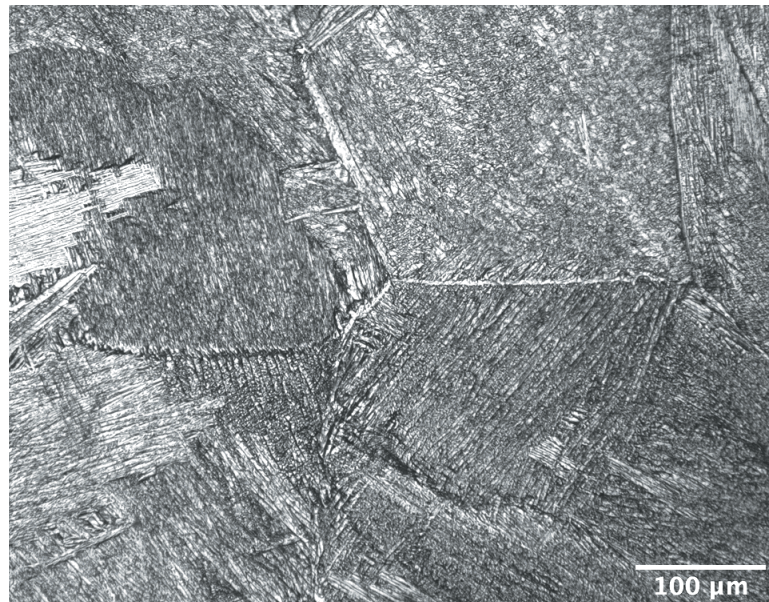


Fig. 1 Example microstructure of the β annealed Ti-6Al-4V plate showing large colonies of aligned α platelets within prior β grains, and grain boundary α delineating the prior β grains: Kroll's etch

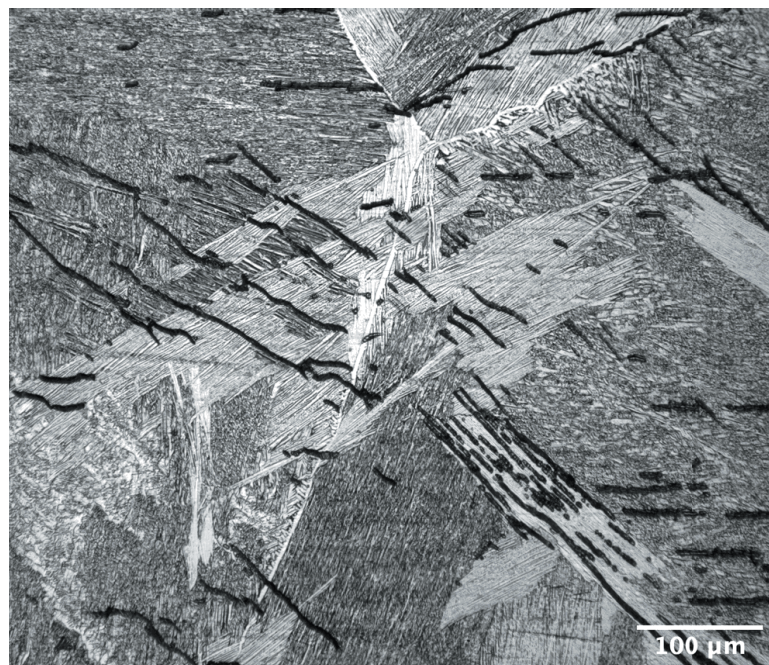
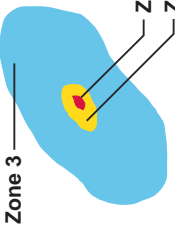
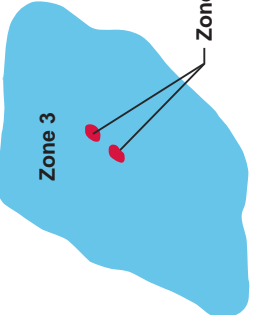
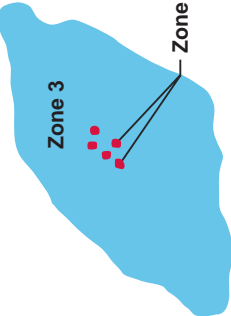
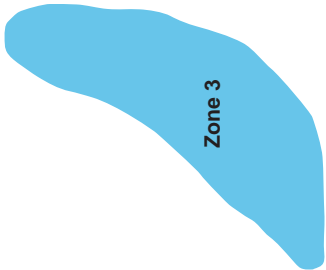



Fig. 2 Microcracks on the cylindrical surface of an LCF-tested specimen taken from the β annealed Ti-6Al-4V plate: Kroll's etch

	Type I Defects		Type II Defects	
	Category 1	Category 2	Category 1	Category 2
Metallurgical observations (typical)	<ul style="list-style-type: none"> Nitrogen stabilized hard alpha zone (zone 2) encasing large spongy-appearing void (zone 1) Alpha case surrounded by enlarged or blocky alpha grains or platelets (zone 3) 	<ul style="list-style-type: none"> Small or no voids (zone 1) No hard alpha zone Large area of nitrogen stabilized enlarged and elongated alpha grains or platelets (zone 3) 	<ul style="list-style-type: none"> Microvoids (zone 1) Low or no elevated nitrogen or oxygen concentration Large area of aluminium stabilized enlarged and elongated alpha grains or platelets (zone 3) 	<ul style="list-style-type: none"> Pure elemental segregation of Ti or Al (zone 3) 
	<ul style="list-style-type: none"> Zone 2 = RC 65-80 Zone 3 = RC 55-70 	RC 45-65	RC 35-45	RC 12
Zone hardness*	All Zones Ellipsoid Shaped as Per the Direction of Work			
Zone shape	All Zones Ellipsoid Shaped as Per the Direction of Work			
Most probable cause	Burnt titanium sponge (source material for ingot production)	Contaminated weldment or contaminated revert material entering ingot	Inclusion drop-in during ingot production	Improperly melted/homogenized alloy or a solidification pipe
Defects in 22 in-service discs	41%	41%	14%	4%
Increasing difficulty to detect by ultrasonic testing 				

* RC = Rockwell hardness "C" scale

Fig. 3 Classification of metallurgical defects causing fatigue failures in titanium alloy aeroengine discs (Costa et al. 1990)

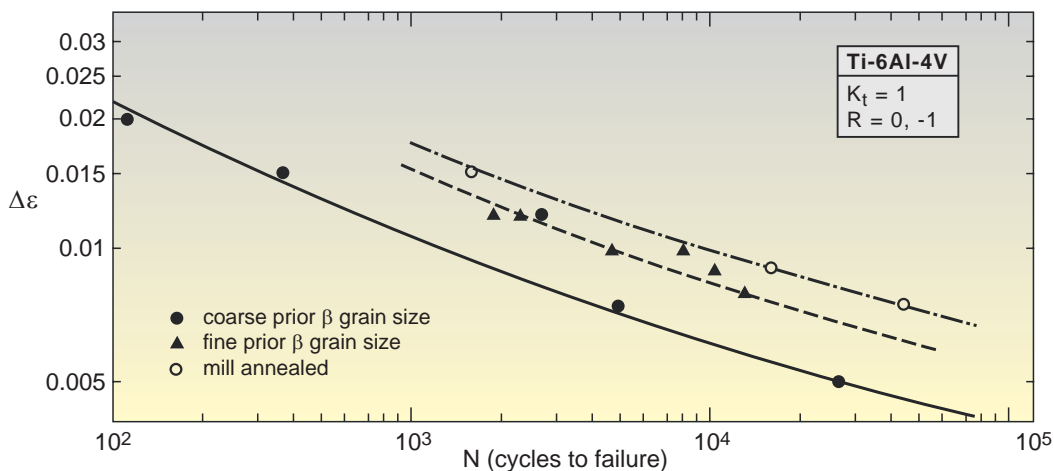


Fig. 4 ϵ - N fatigue curves for Ti-6Al-4V in three microstructural conditions: fully lamellar (coarse prior β grain size), fully lamellar (fine prior β grain size) and mill annealed (Evans 1999)

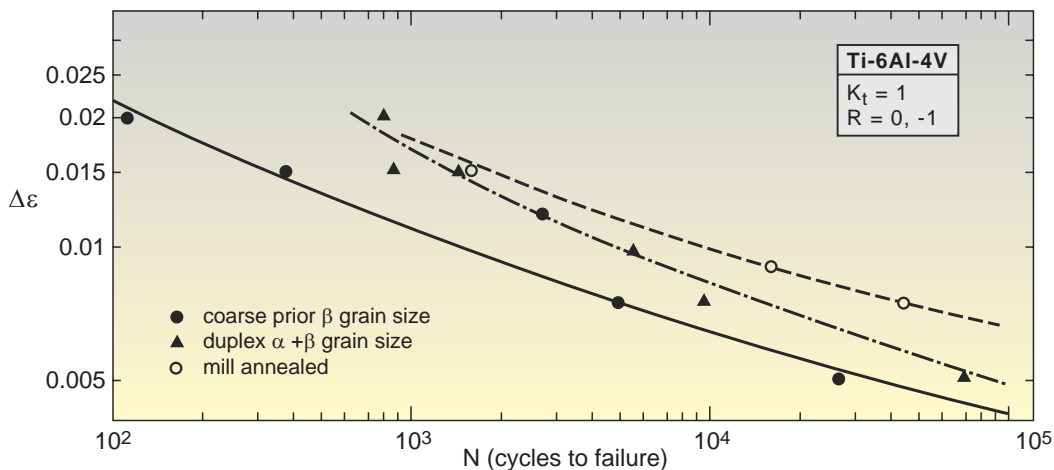


Fig. 5 ϵ - N fatigue curves for Ti-6Al-4V in three microstructural conditions: fully lamellar (coarse prior β grain size), duplex (82% α) and mill annealed (Evans 1999)

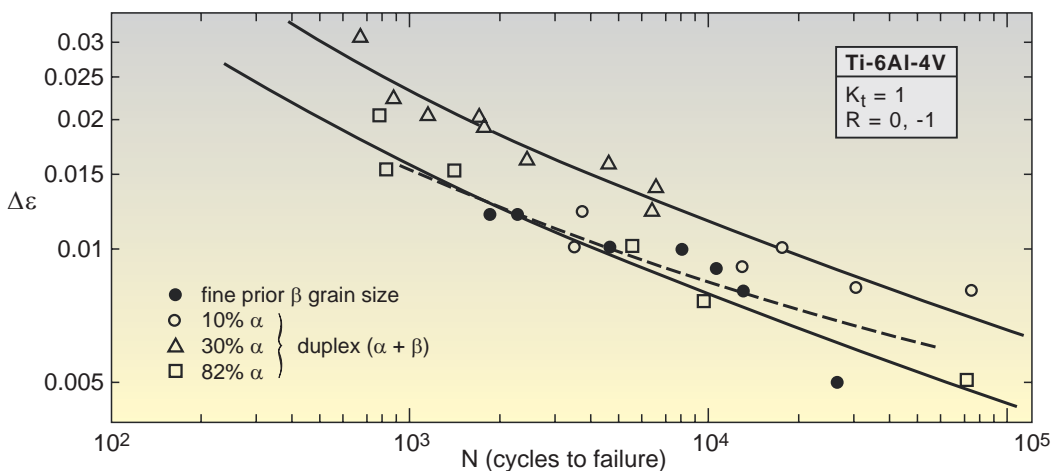


Fig. 6 ϵ - N fatigue curves for Ti-6Al-4V in four microstructural conditions: fully lamellar (fine prior β grain size) and duplex (10% α , 30% α , 82% α) (Evans 1999)

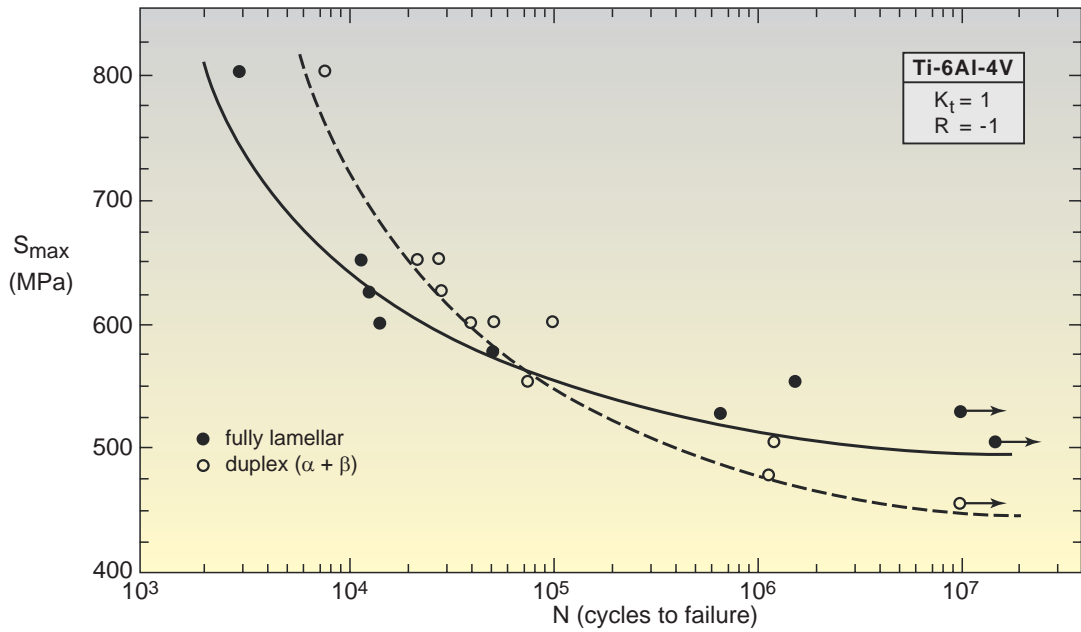


Fig. 7 S–N fatigue curves for Ti-6Al-4V in two microstructural conditions: fully lamellar and duplex (35% α) (Hines and Lütjering 1999)

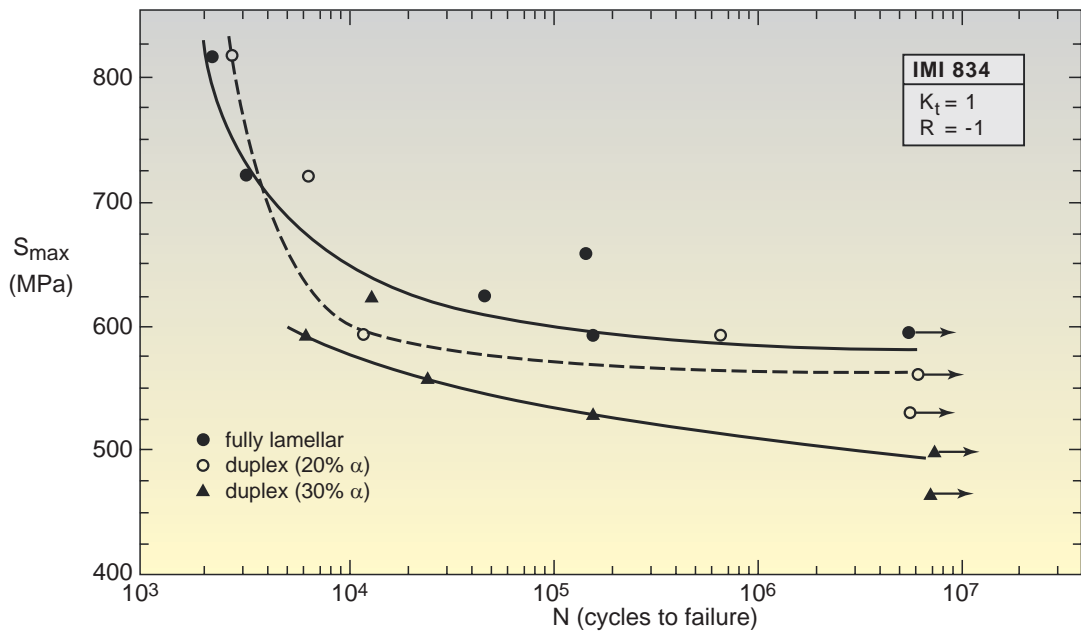


Fig. 8 S–N fatigue curves for IMI 834 (Ti-5.8Al-log4.0Sn-3.5Zr-0.7Nb-0.5Mo-0.35Si-0.06C) in three microstructural conditions: fully lamellar and duplex (20% α, 30% α) (Lütjering et al. 1999)

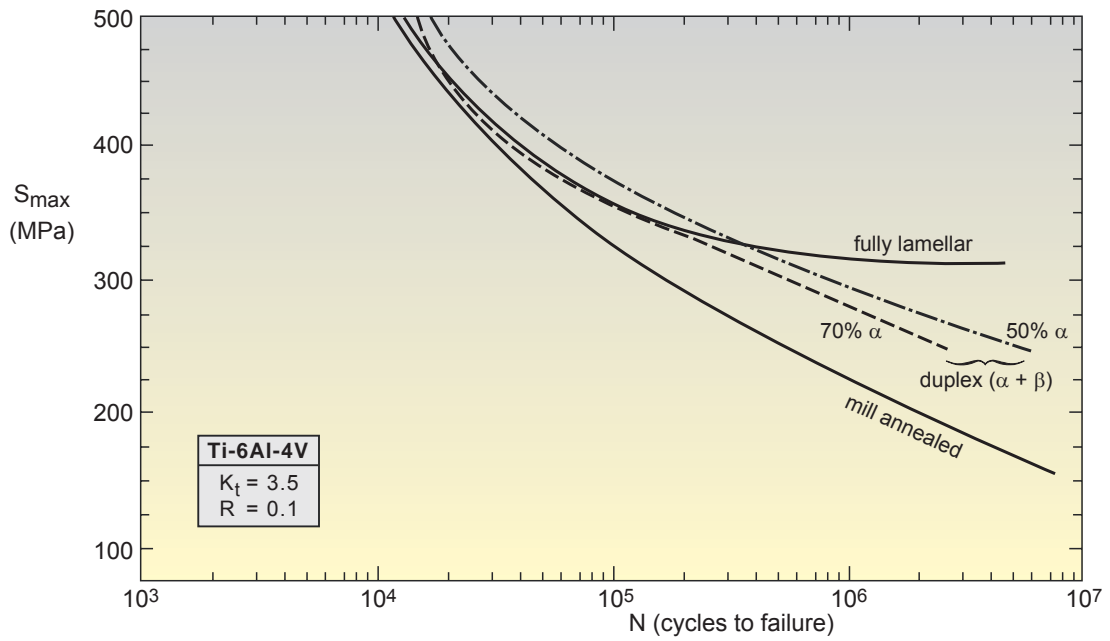


Fig. 9 S–N notched fatigue curves for Ti-6Al-4V plate in four microstructural conditions: fully lamellar, duplex (50% α , 70% α) and mill annealed (Eylon and Pierce 1976)

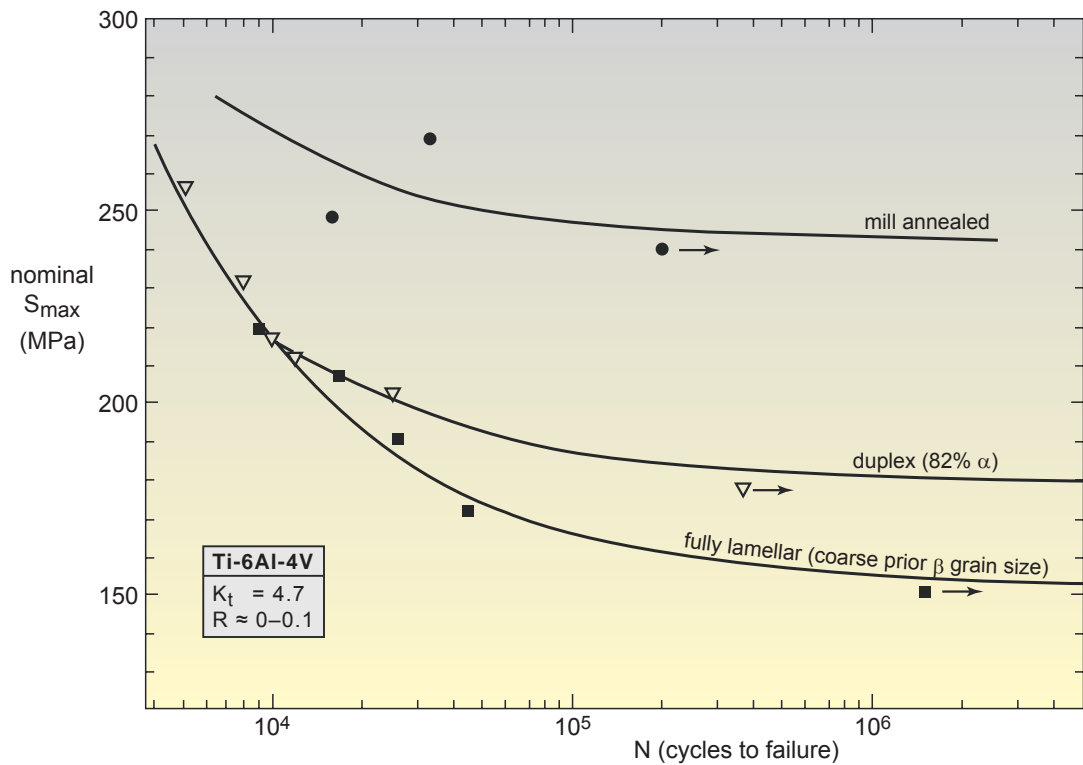


Fig. 10 S–N notched fatigue curves for Ti-6Al-4V plate in three microstructural conditions: fully lamellar, duplex (82% α) and mill annealed (Evans 1999)

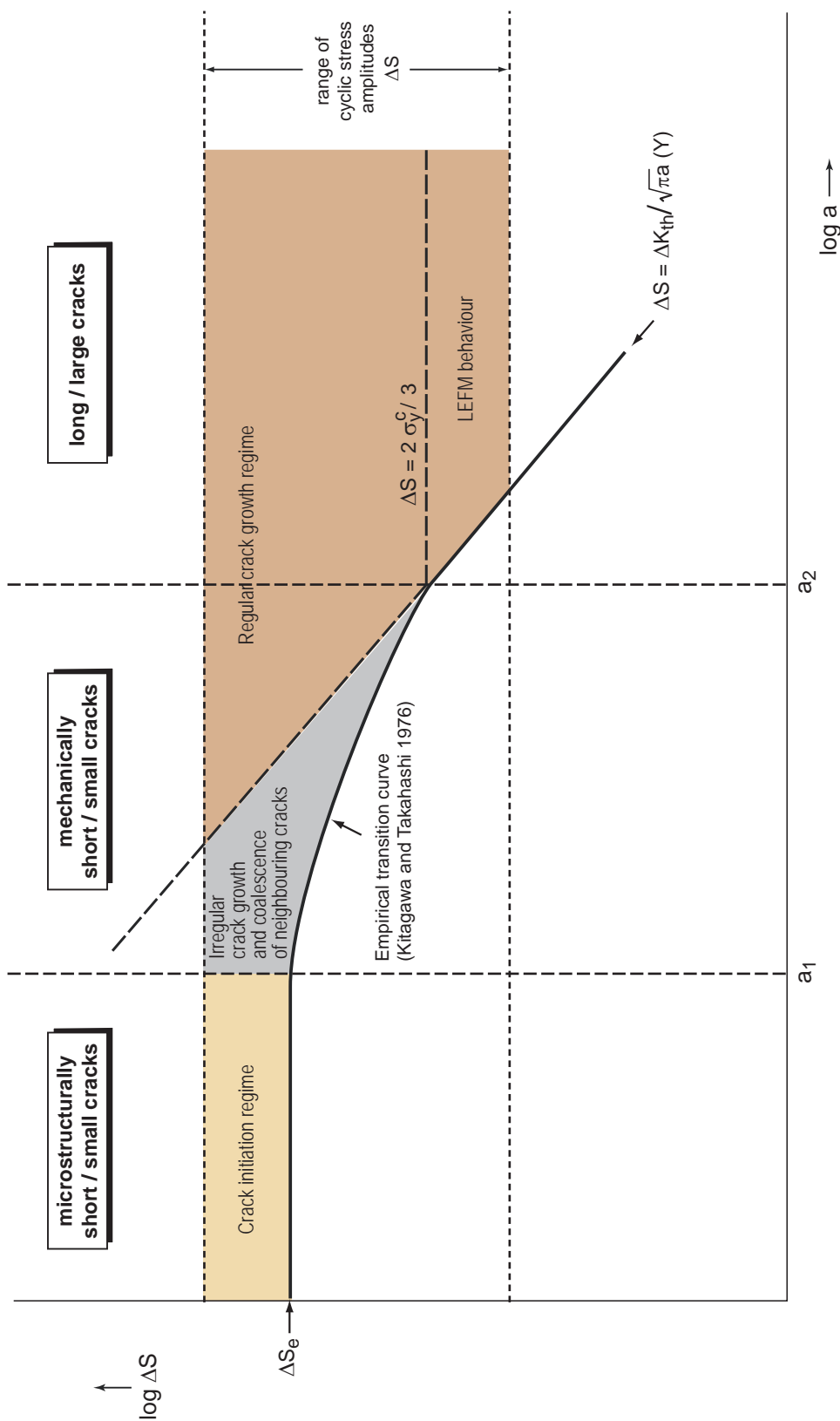


Fig. 11 Dependence of fatigue crack behaviour (initiation, irregular growth and coalescence, sustained growth) on cyclic stress amplitudes, ΔS , and crack sizes, a . ΔS_e = fatigue stress range endurance limit; ΔK_{th} = fatigue crack growth threshold for long/large cracks; Y = geometric factor dependent on crack shape and size and specimen or component shape and size; σ_y^c = cyclic yield stress

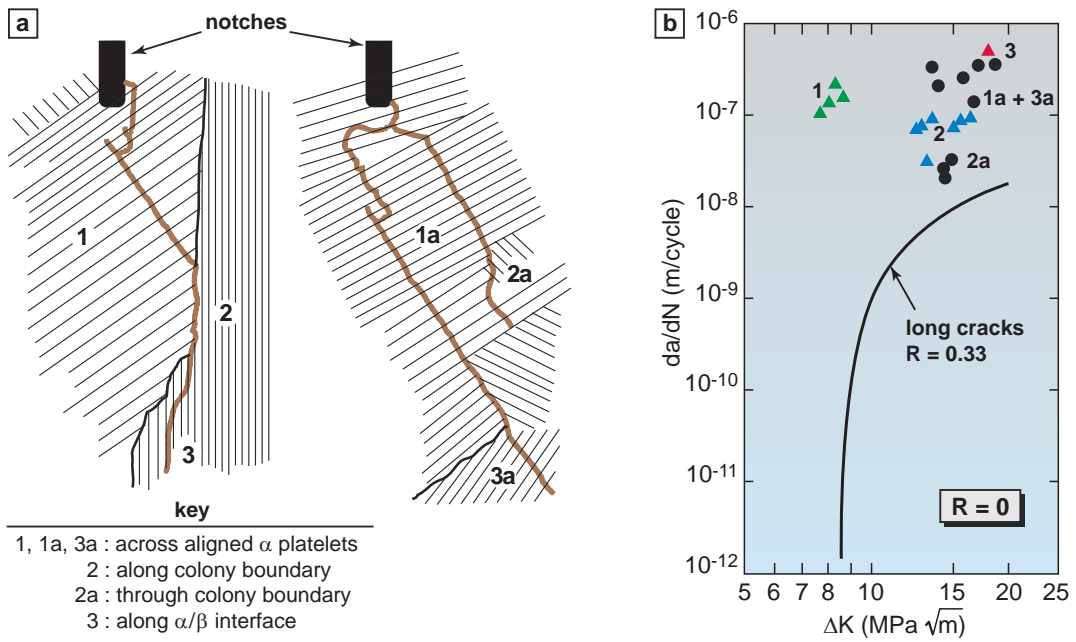


Fig. 12 Microstructurally short fatigue crack growth in IMI 685: (a) sketches of actual crack paths; (b) crack growth rates compared to a long crack growth rate curve (Hicks and Brown 1982)

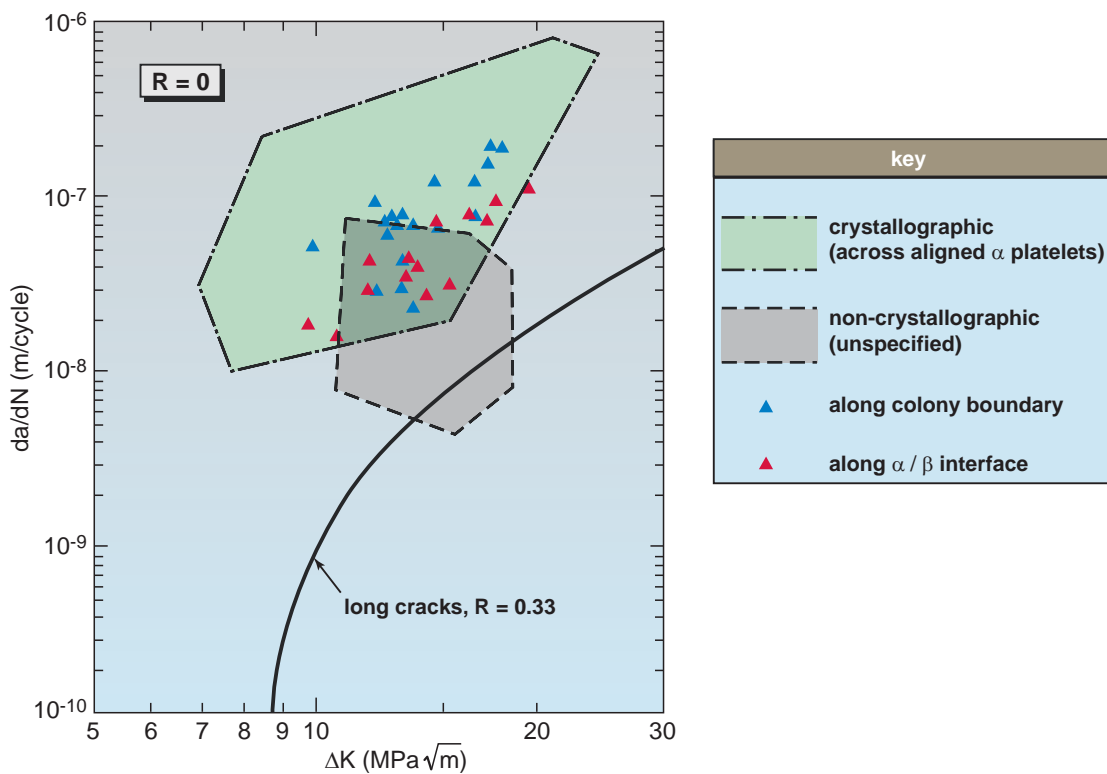


Fig. 13 Microstructurally short fatigue crack growth in IMI 685. After Brown and Hicks (1983) and Hicks et al. (1983a)

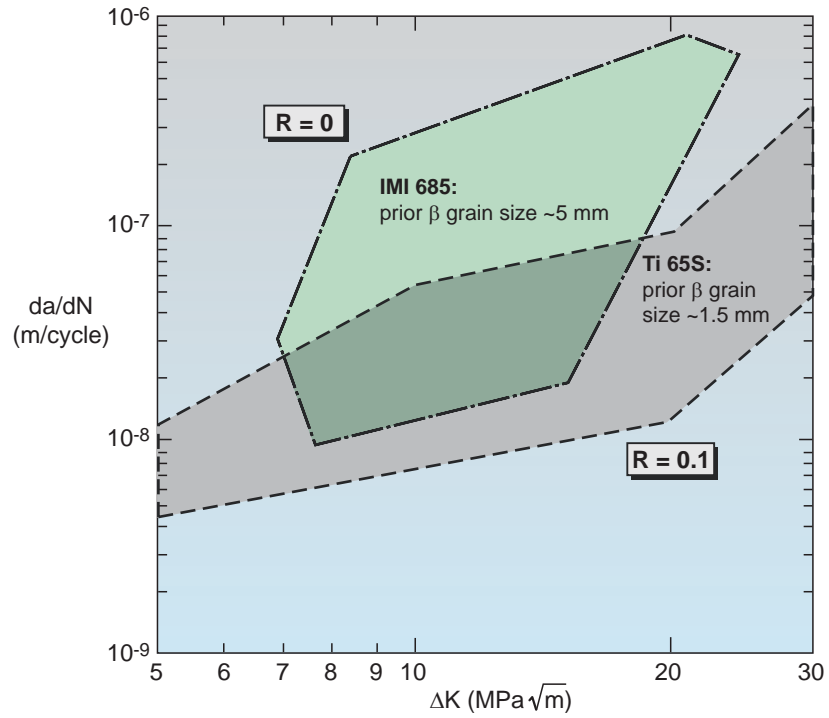


Fig. 14 Microstructurally short fatigue crack growth across aligned α platelets in IMI 685 and Ti65S. After Brown and Hicks (1983) and Hastings et al. (1987)

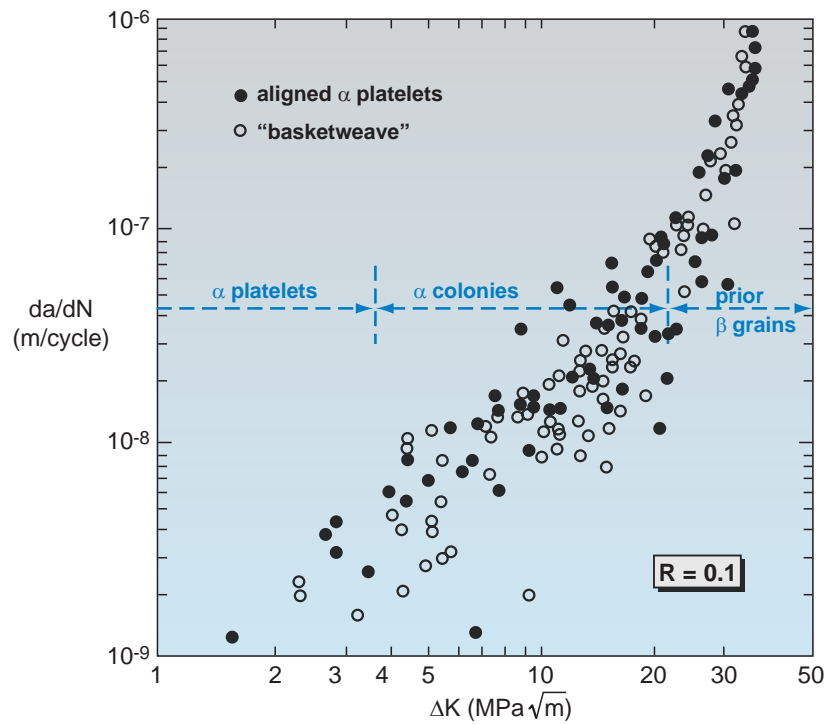


Fig. 15 Microstructurally short fatigue crack growth in Ti65S. After Hastings et al. (1987)

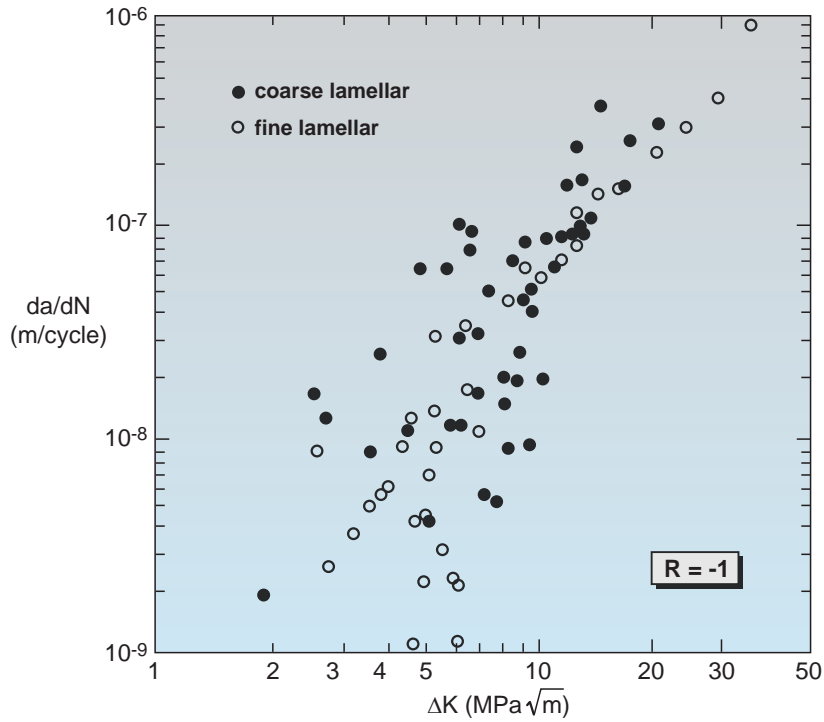


Fig. 16 Microstructurally short fatigue crack growth in Ti-6Al-4V. After Wagner and Lütjering (1987)

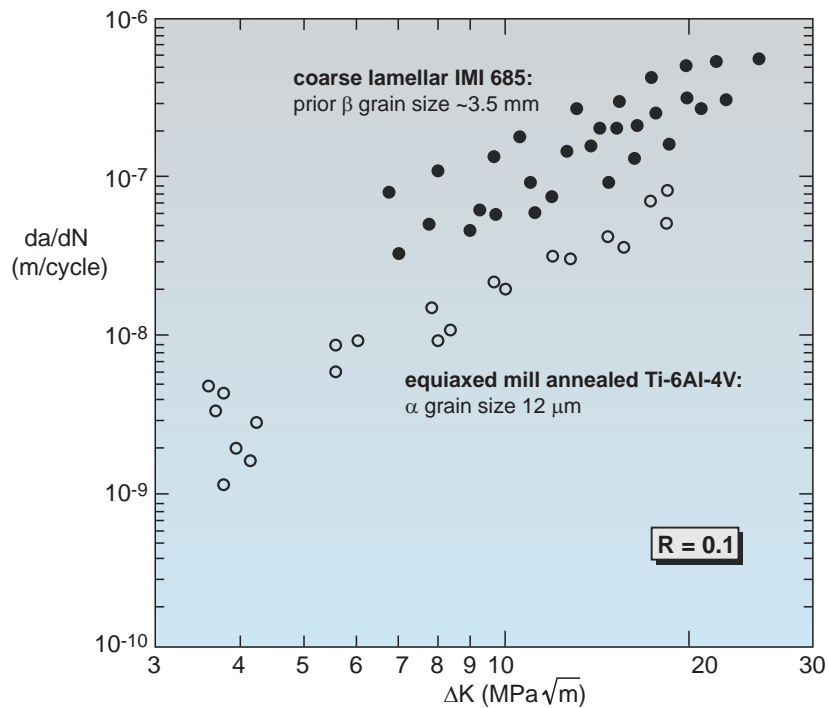


Fig. 17 Microstructurally short (IMI 685) and mechanically short (Ti-6Al-4V) fatigue crack growth comparisons (Hicks and Brown 1984)

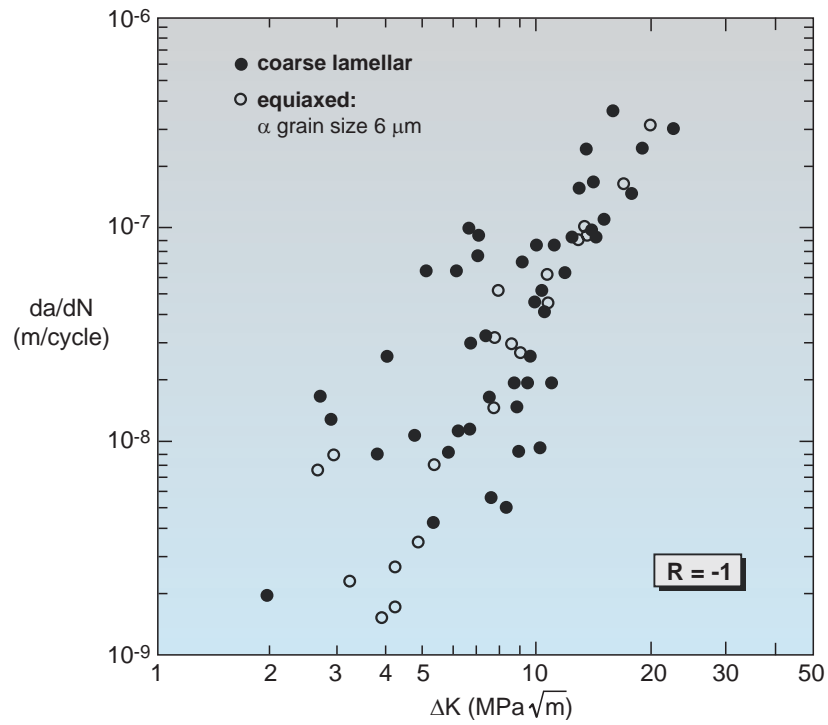


Fig. 18 Microstructurally short (coarse lamellar) and mechanically short (equiaxed) fatigue crack growth in Ti-6Al-4V. After Wagner and Lütjering (1987)

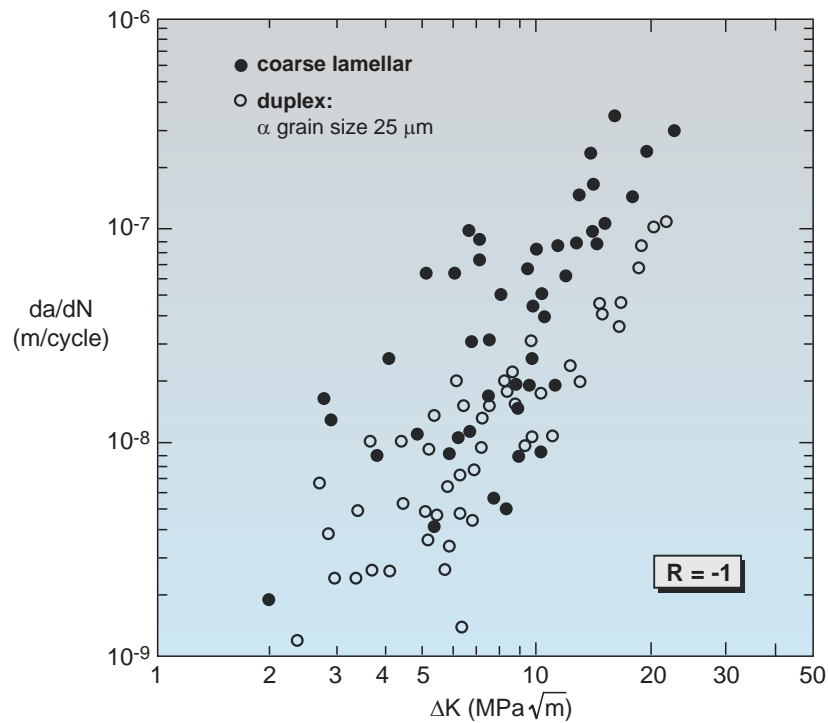


Fig. 19 Microstructurally short (coarse lamellar) and mechanically short (duplex) fatigue crack growth in Ti-6Al-4V. After Wagner and Lütjering (1987)

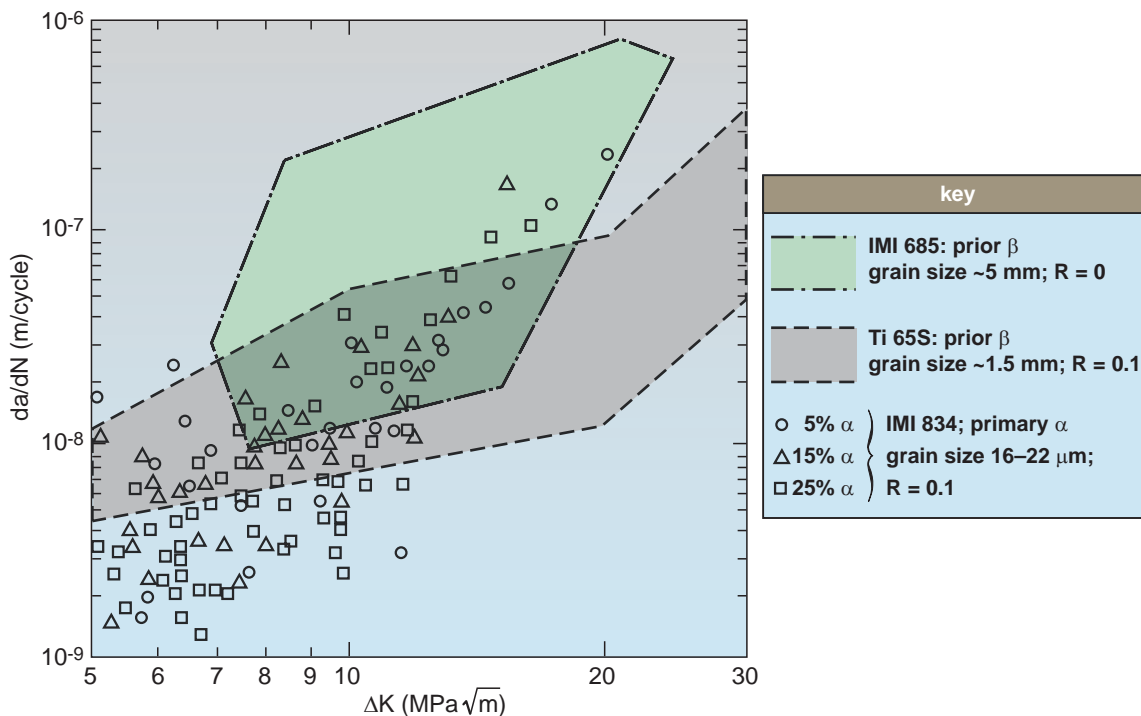


Fig. 20 Microstructurally short (IMI 685 and Ti65S) and mechanically short (IMI 834) fatigue crack growth comparisons. After Brown and Hicks (1983), Hastings et al. (1987) and Dowson et al. (1992)

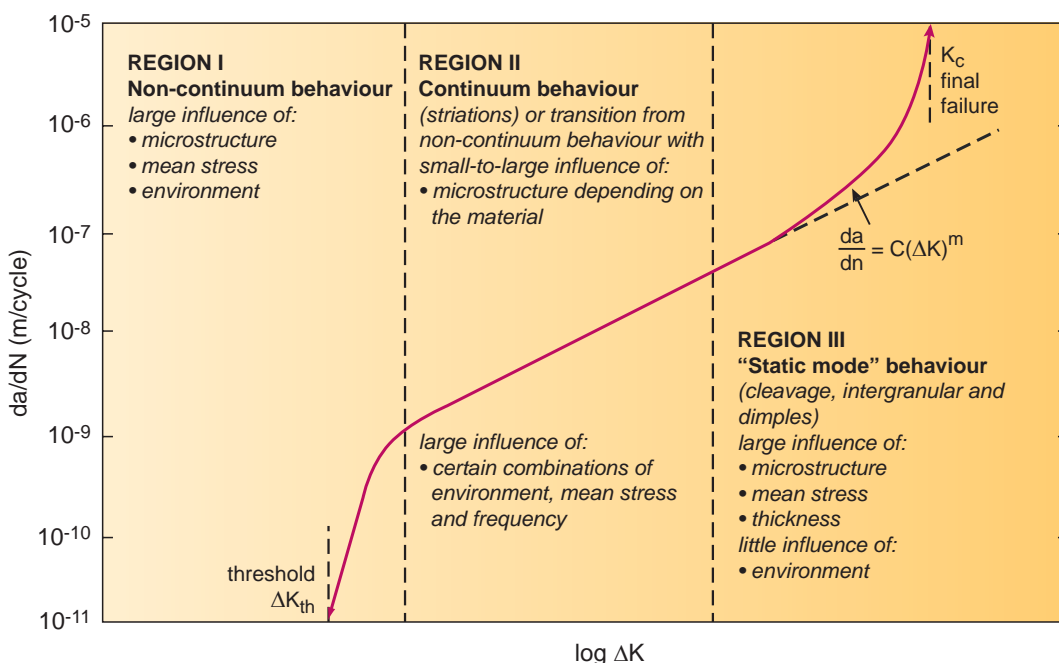


Fig. 21 Characteristics of the long/large fatigue crack growth rate curve $\log da/dN$ versus $\log \Delta K$ (Ewalds and Wanhill 1984)

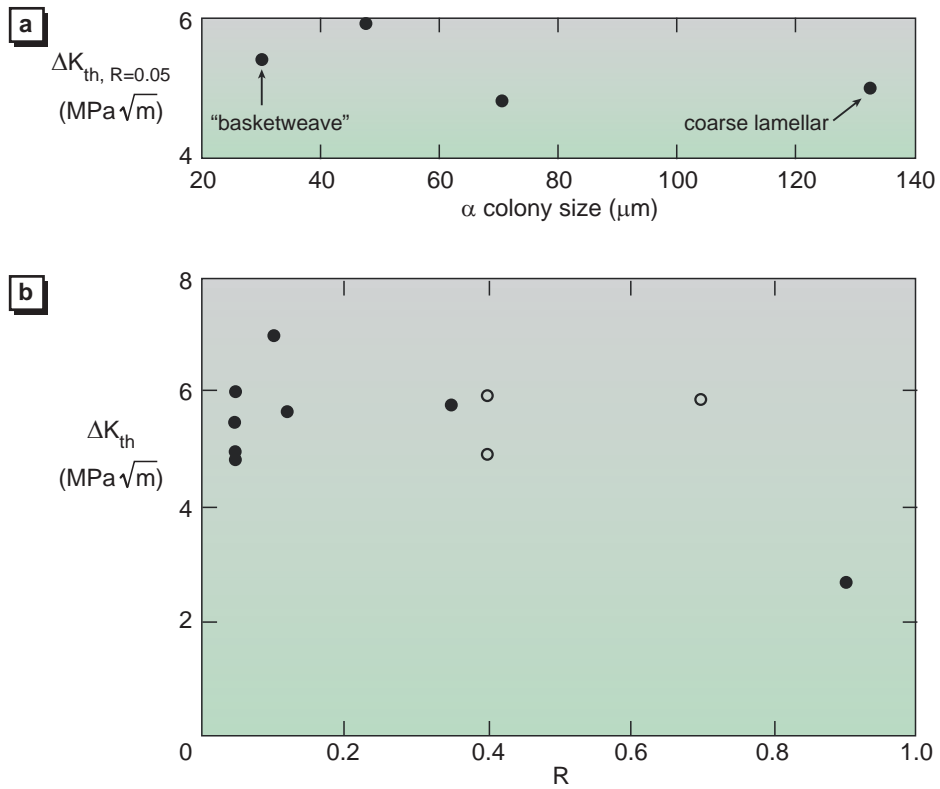


Fig. 22 Dependence of β annealed Ti-6Al-4V ΔK_{th} on (a) α colony size and (b) stress ratio, R . Solid symbol (●) data from Irving and Beevers (1974), Lütjering and Wagner (1987) and Ravichandran (1991); open symbol (○) data from NLR tests (2008)

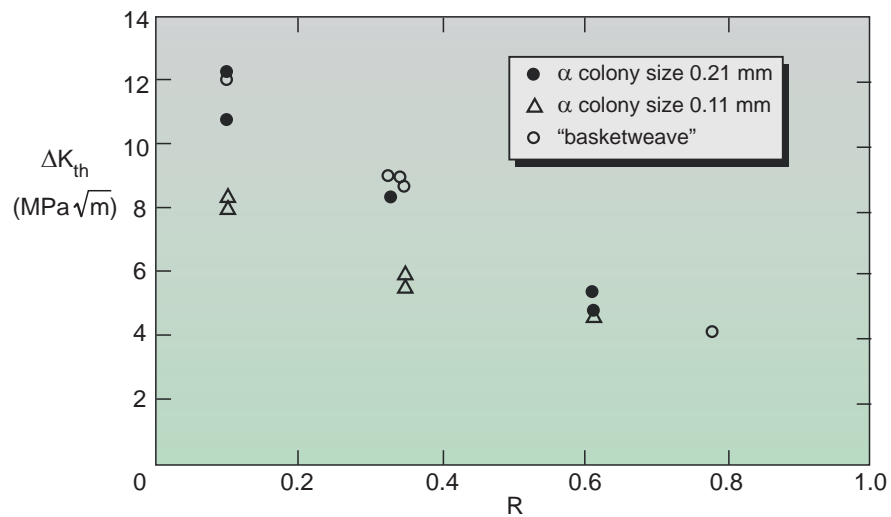


Fig. 23 Dependence of β processed and annealed IMI 685 ΔK_{th} on stress ratio, R (Hicks et al. 1983b)

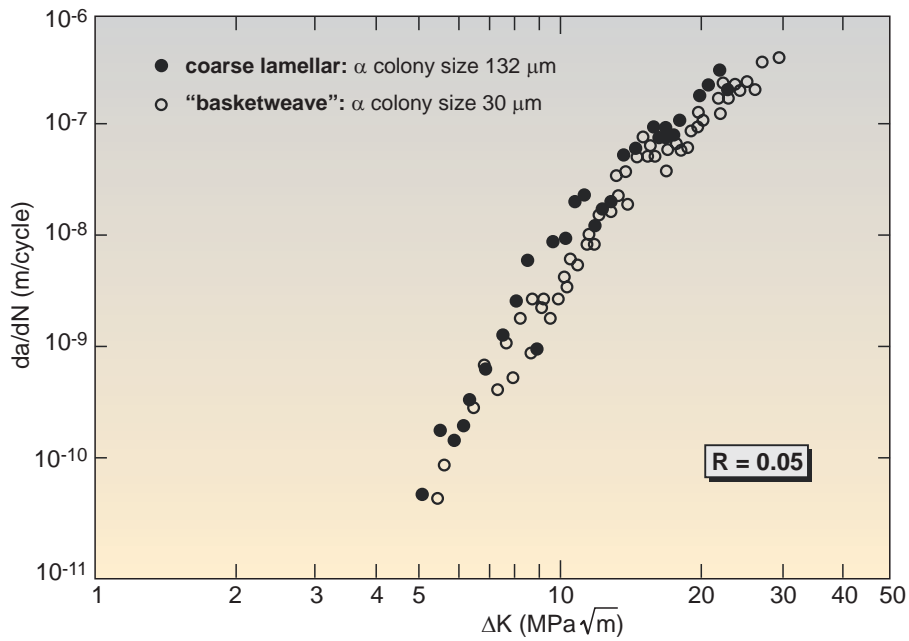


Fig. 24 Dependence of β annealed Ti-6Al-4V regions I and II long/large fatigue crack growth on α colony size. After Ravichandran (1991)

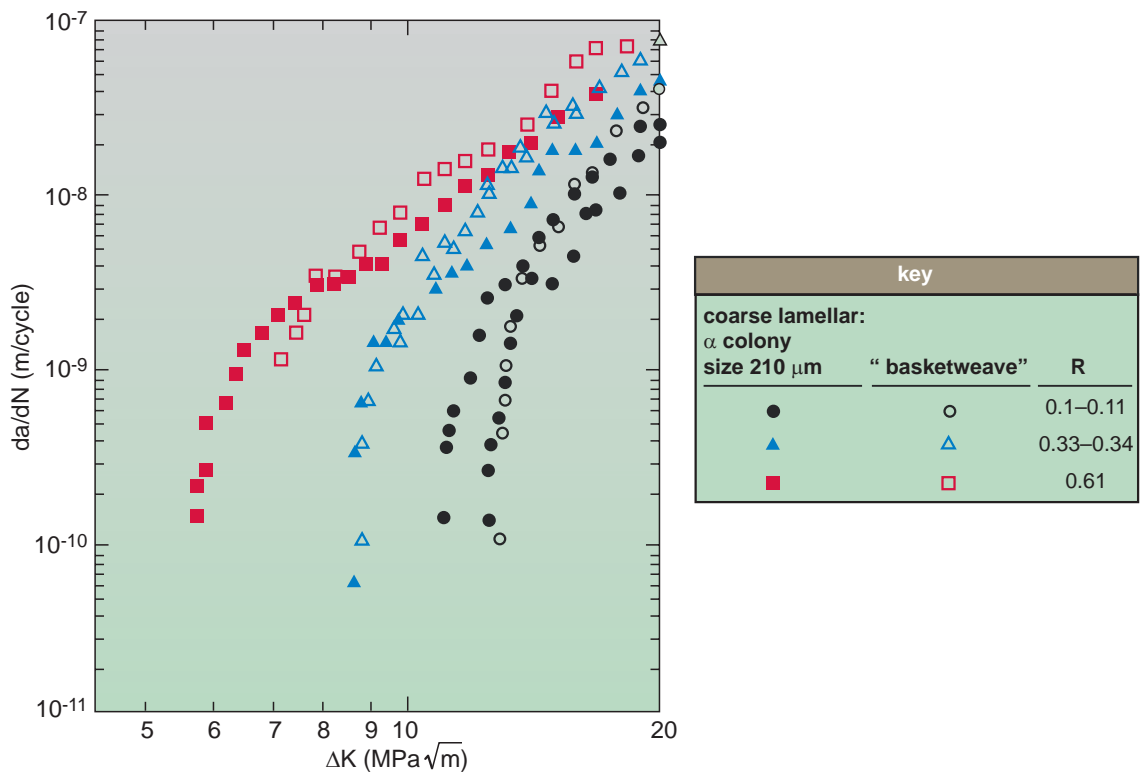


Fig. 25 Dependence of β processed and annealed IMI 685 regions I and II long/large fatigue crack growth on final microstructure (coarse lamellar and "basketweave") and stress ratio, R . After Hicks et al. (1983b)

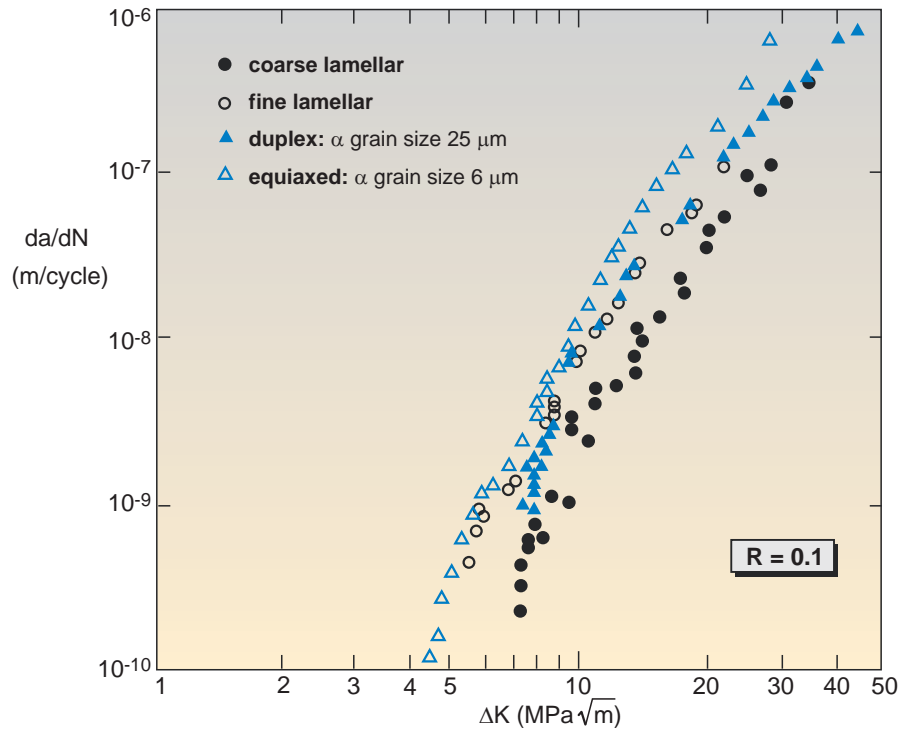


Fig. 26 Dependence of Ti-6Al-4V regions I and II long/large fatigue crack growth on microstructure. After Wagner and Lütjering (1987)

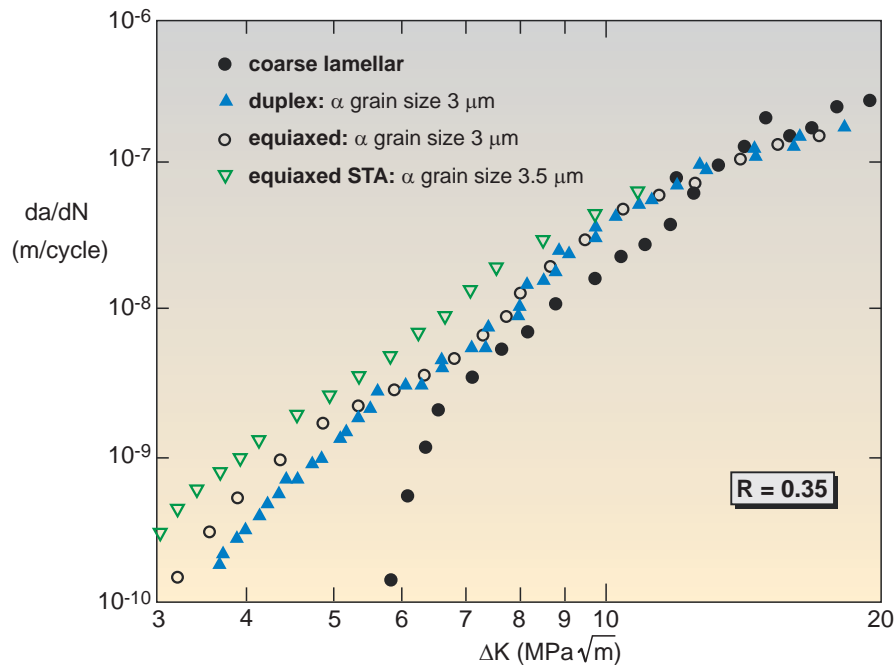


Fig. 27 Dependence of Ti-6Al-4V regions I and II long/large fatigue crack growth on microstructure (Irving and Beevers 1974). STA = ($\alpha+\beta$) Solution Treated and Aged

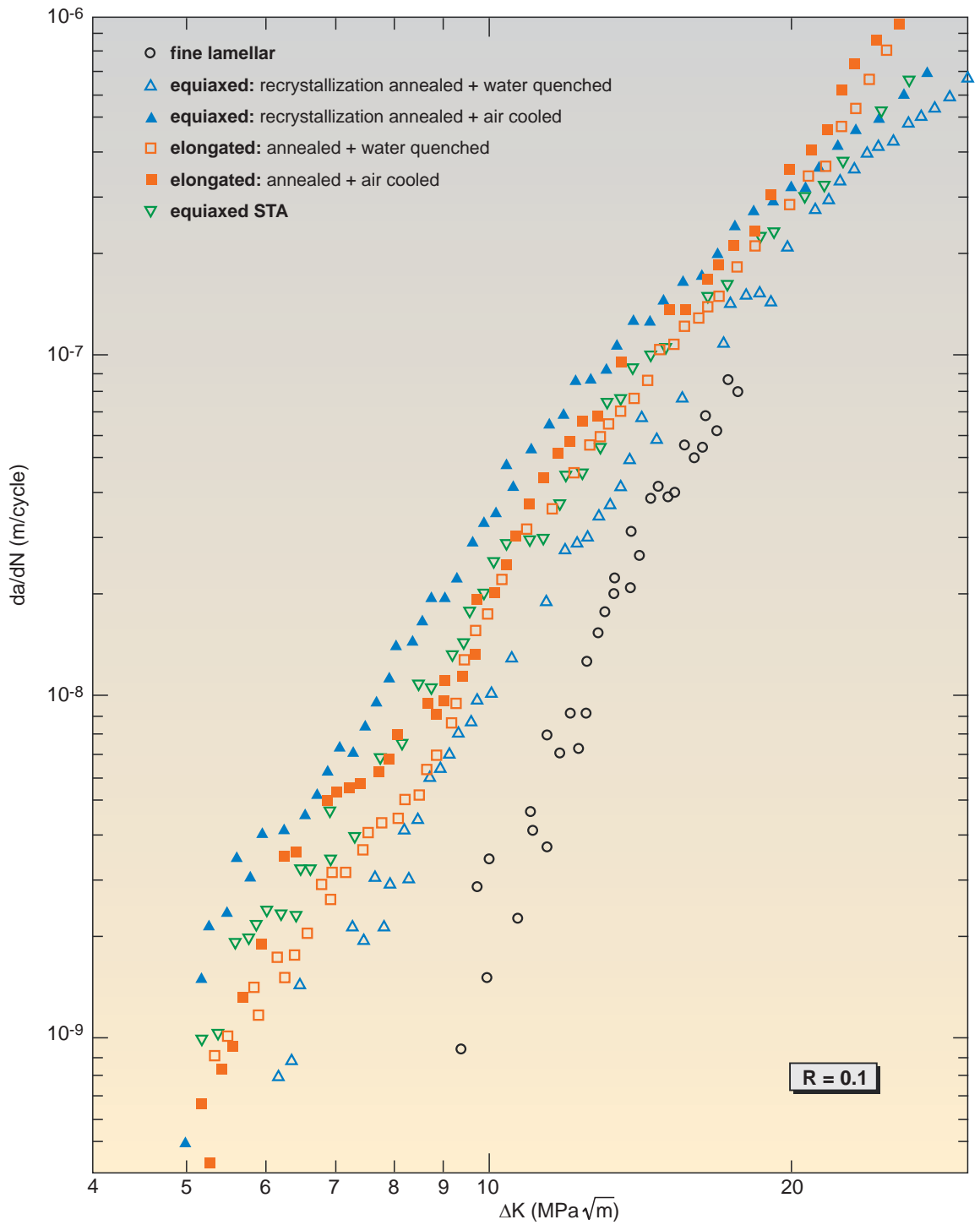


Fig. 28 Dependence of Ti-6Al-4Mo-2Zr-0.2Si regions I and II long/large fatigue crack growth on microstructure (Saxena and Radhakrishnan 1998). STA = ($\alpha+\beta$) Solution Treated and Aged

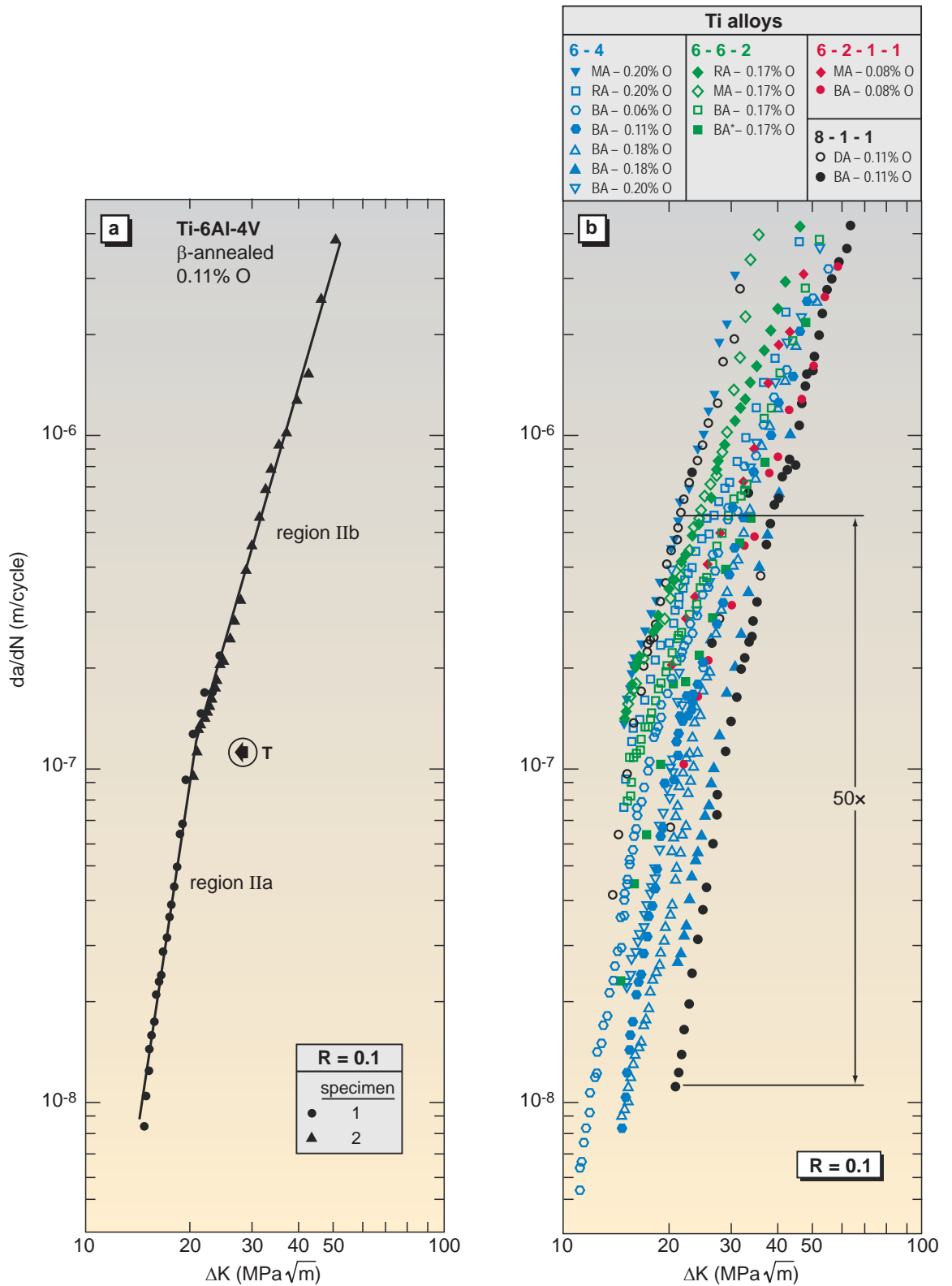


Fig. 29 Examples of region II fatigue crack growth for (a) a β annealed Ti-6Al-4V ELI plate and (b) several titanium alloys in different heat treatment conditions (Yoder et al. 1978, 1979)